



Modeling *Drosophila suzukii*'s Population using SIT

The effectiveness of mixed release

Student: Belkhayate Taha

Supervisors: van Oudenhove Louise
Mailleret Ludovic
Courtois Marine

Collège STEE - Université de Pau et des Pays de l'Adour (UPPA)
Institut Sophia Agrobiotech - INRAE Sophia-Antipolis
September 2023



Contents

	Page
<i>List of Figures</i>	III
<i>Declaration</i>	VI
<i>Abstract</i>	VII
1 Introduction	1
1.1 Institut Sophia Agrobiotech and The M2P2 team	1
1.2 General framework	1
1.3 The Sterile Insect Technique (SIT)	2
1.4 The aim of the internship	3
2 Mathematical Modeling of <i>Drosophila Suzukii</i>'s population	5
2.1 First Basic Model of <i>D. suzuki</i> 's population (3 compartments)	6
2.1.1 Male abundance $M \geq F$	9
2.1.2 Male scarcity $M < F$	11
2.2 Second Model (4 compartments) Incorporating Conditional Mating Abilities for Males and Females	14
2.2.1 Male abundance $M\gamma > V$	15
2.2.2 males scarcity $M\gamma < V$	18
3 Modeling the SIT releases	23
3.1 Modeling of SIT with only sterile males releases	23
3.1.1 Inserting sterile males in the basic model	24
3.1.2 6 compartments simplified model	30
3.1.3 Model Incorporating the re-mating Ability in the 6 Compartments model	34
3.2 Releasing sterile Females and Males	39
3.2.1 Embracing sterile Females and Males releases in the Basic Model	39
3.2.2 Simulation	44
3.2.3 Releasing the Entire Population 7-compartment model.	45
3.2.4 The 7 compartments model with remating ability	47
3.2.5 Releasing the entire Population with preferences.	48
4 The effectiveness of releasing sterile females alongside sterile males vs. only males release	51
4.1 Comparing the release strategies and their effectiveness in the case of the three cohort model 3.1, and 3.7	51
4.2 Comparison of the release strategy and its effectiveness in the case of all the hypotheses included systems 3.5, and 3.12	53
4.3 Conclusion and Discussion	54

<i>Bibliography</i>	58
---------------------	----

List of Figures

	Page
1.1 Spread of <i>D. suzukii</i> worldwide in the 09-02-2015 (source: EPPO Global Database ¹ .)	2
1.2 Spread of <i>D. suzukii</i> worldwide Last updated: 22-05-2023 (source: EPPO Global Database)	2
1.3 Diagram of the main steps of the sterile insect technique ^[1]	3
2.1 Diagram of the population model for TIS <i>Drosophila suzukii</i> , corresponding to the system of equations 2.1.	6
2.2 Simulation of <i>Drosophila suzukii</i> population evolution, with $L = 0$, $M = 1$ and $F = 1$ as an initial condition for both sets of Data	13
2.3 Gender Balance of <i>D. suzukii</i> : Males vs Females Numbers in the case of the 2.1	14
2.4 Diagram of the population model of <i>Drosophila suzukii</i> , corresponding to the system of equations 2.7	15
2.5 Population Dynamics over Time: in the Model 3.1 without Constraints, $L = 0$, $M = 1$, $V = 1$, $F = 0$	21
2.6 Sex ratio of <i>D. suzukii</i> : Males vs. Females Numbers in the case of the 3.1 model, starting from $M = 1$, and $F = 1$	22
3.1 Diagram of the population model of <i>Drosophila suzukii</i> , corresponding to the system of equations 3.1 with sterile males releases	24
3.2 Intersection between The number of sterile Males released and the number of Larvas at the equilibrium (First set of Data)	25
3.3 Intersection between The number of sterile Males released and the number of Larvas at the equilibrium (second set of Data)	25
3.4 Bifurcation diagram of the stability points for the equilibrium points with SIT as a function of the number of sterile males M_s first data	28
3.5 Bifurcation diagram of the stability points for the equilibrium points with SIT as a function of the number of sterile males M_s second data	28
3.6 Simulation of the population evolution of <i>Drosophila suzukii</i> , in the TIS model 3.1, with continuous releases of sterile males ($M_S = 1200$) with an initial condition $L = 1000$, $M = 0$, and $F = 0$	29
3.7 Simulation of the population evolution of <i>Drosophila suzukii</i> , in the TIS model 3.1, with continuous releases of sterile males ($M_S = 10000$) with an initial condition $L = 1000$, $M = 0$, and $F = 0$	29
3.8 Diagram of the population model for TIS <i>Drosophila suzukii</i> , corresponding to the system of equations 3.3	30
3.9 Bifurcation diagram of the stability points for the equilibrium points with SIT as a function of the number of sterile males M_s first data	34
3.10 Bifurcation diagram of the stability points for the equilibrium points with SIT as a function of the number of sterile males M_s second data	34
3.11 Diagram of the population model for TIS <i>Drosophila suzukii</i> , corresponding to the system of equations 3.5	35

3.12	Intersection of Larva equilibrium points curve with one of the males release complex model	36
3.13	Intersection of Larva equilibrium points curve with one of the males release complex model	36
3.14	Bifurcation diagram of the stability points for the equilibrium points with SIT as a function of the number of sterile males M_s first data	37
3.15	Bifurcation diagram of the stability points for the equilibrium points with SIT as a function of the number of sterile males M_s second data	37
3.16	Population dynamics with Releasing Ms = 80000 Males continuously , $M = 2000$ $V = 2000$	38
3.17	Intersections between the two graphs $\zeta_1(L)$ (in red) and Γ for different values of the released population $N = 500$ (blue), $N = 724$ (orange), and $N = 800$ green. The red dots represent the intersection points. (first data set)	41
3.18	Intersections between the graphs of $\zeta(L)$ (in red) and Γ for different values of the released population $N = 10000$ (blue), $N = 22870$ (orange), and $N = 25000$ green. The red dots represent the intersection points. (second data set)	41
3.19	Equilibrium points and its stability in the function of the number of released population $N = F_s + M_s$ and $F_s = M_s$, first data set	44
3.20	Equilibrium points and its stability in the function of the number of released population $N = F_s + M_s$ and $F_s = M_s$, second data	44
3.21	Simulation of the population evolution of <i>Drosophila suzukii</i> , in the TIS model 3.7, with continuous releases of sterile males and females ($M_s = F_s = 500$, and initial conditions of $L = 1000$, $M = F = 0$)	45
3.22	Diagram of the population model for SIT applied to <i>Drosophila Suzukii</i> , corresponding to the system of equations 3.11	46
3.23	Simulation of the population evolution of <i>Drosophila suzukii</i> , in the TIS model 3.11, with continuous releases of sterile males and females ($M_s = F_s = 7500$, and initial conditions of $L = 0$, $M = V = 2000$ and $F = S = 0$)	46
3.24	Diagram of the population model for TIS <i>Drosophila suzukii</i> , corresponding to the system of equations 3.12	47
3.25	Simulation of the population evolution of <i>Drosophila suzukii</i> , in the TIS model 3.11, with continuous releases of sterile males and females ($M_s = F_s = 7500$, and initial conditions of $L = 0$, $M = V = 2000$ and $F = S = 0$)	48
3.26	Intersexual Attractiveness of the population, grey represents steriles	49
3.27	Simulation of the population evolution of <i>Drosophila suzukii</i> , in the TIS model 3.12 with preferences, with continuous releases of sterile males and females ($M_s = F_s = 7500$, and initial conditions of $L = 0$, $M = V = 2000$ and $F = S = 0$)	50
4.1	Bifurcation diagram of the stability points for the equilibrium points with SIT as a function of the number of sterile males M_s first data	51
4.2	Bifurcation diagram of the stability points for the equilibrium points with SIT as a function of the number of sterile males M_s second data	51
4.3	Equilibrium points and its stability in the function of the number of released population $N = F_s + M_s$ and $F_s = M_s$, first data set	52
4.4	Equilibrium points and its stability in the function of the number of released population $N = F_s + M_s$ and $F_s = M_s$, second data	52
4.5	Minimum number of sterile individuals released required to reach eradication in each strategy in the first dataset	52
4.6	Minimum number of sterile individuals released required to reach eradication in each strategy in the first dataset	52
4.7	Simulation of the population evolution of <i>Drosophila suzukii</i> , in the TIS model 3.5, with continuous releases of sterile males ($M_s = 80000$, and initial conditions of $L = 0$, $M = V = 2000$ and $F = S = 0$)	53

4.8	Simulation of the population evolution of <i>Drosophila suzukii</i> , in the TIS model 3.11, with continuous releases of sterile males and females ($M_s = F_s = 40000$, and initial conditions of $M = V = 2000$, and $L = F = S = 0$)	53
-----	---	----

Declaration

I hereby declare that the work presented in this master thesis is entirely my own and that I did not use any other sources and references than the listed ones. I have marked all direct or indirect statements from other sources contained therein as quotations. Neither this work nor significant parts of it were part of another examination procedure. The electronic copy is consistent with all submitted copies.

Pau (France), September 2023

Abstract

The invasive fruit fly, *Drosophila suzukii*, poses a significant threat to global agriculture by causing substantial damage to various fruit crops (e.g. berries such as Strawberries, Blueberries, Cherries, Raspberries, and Blackberries, also Grapes, Peaches, and Nectarines). In^[2] they assessed a decrease in the California berry industry revenues by 37% for raspberries and by 20% for processed strawberries. To find a solution for such a pest there is a wide array of pest management techniques available, each tailored to address specific pest-related challenges. The Sterile Insect Technique (SIT), is one of these solutions, as a pest management strategy and a friendly environmental method. SIT relies on the mass rearing and continuous release of sterilized insects in huge numbers into the target pest population, to decrease the number of matings that could lead to offspring

The aim of this study is to create a mathematical ODE model that assesses the efficacy of the Sterile Insect Technique (SIT) in controlling *D. Suzukii* populations while using two strategies, the release of males only and the release of both males and females, and comparing their effectiveness.

Some authors have shown that releases of males and females are more or equally effective than releases of males alone^[3] and^[4]. Others have shown that², on the contrary, releasing both males and females reduces the effectiveness of the sterile insect technique^[5] and^[6]. This is from where it comes the necessity of this study.

Through a series of analytical studies and simulations of many different models, that have been involved gradually, the release of both sterile males and females, as opposed to only sterile males release, could offer enhanced efficacy in suppressing *D.Suzukii*. Yet, in order to suppress the population we still need an extensive amount of releases of both populations alongside maintaining a minimal presence of the wild population.

This work contributes to the development of effective strategies for controlling *D. Suzukii* populations using the sterile insect technique. The model's predictions and insights can guide policymakers and pest management practitioners in designing and optimizing SIT programs, leading to sustainable and environmentally friendly pest control practices in agriculture.

²Note that these studies were not carried out on the same species

Introduction

1.1 Institut Sophia Agrobiotech and The M2P2 team

Institut Sophia Agrobiotech³ is an international research institute funded by INRAE, Université Côte d’Azur, and CNRS. The main research themes developed concern the study of the functioning of interactions between plants, pests, and symbionts, and their dynamics in time and space. To achieve this, the Institute brings together strong skills in comparative, evolutionary, and functional genomics, community ecology, and agronomy. The Institut Sophia Agrobiotech’s ambition is to meet some of the challenges facing agronomic research in the field of ecological management of agrosystems, by integrating this knowledge into the development of innovative agronomic strategies (plant resistance, integrated protection, and biological control) that are more respectful of the environment and human health.

The Models and Methods for Plant Protection team (M2P2) is one of the research teams of the Institut Sophia Agrobiotech (ISA, UMR INRAE, Université Côte d’Azur et CNRS). It specializes in the development of research programs based on the concerted use of theoretical and experimental approaches to address specific plant protection issues, from the individual level to populations and agroecosystems. In this way, the team aims to make plant protection more respectful of the environment through the development of innovative strategies for the ecological control of crop pests and diseases.

1.2 General framework

Drosophila suzukii (Matsumura) (Diptera: Drosophilidae) also known as the spotted-wing Drosophila (SWD), is a pest that originated from Southeast Asia. In the last few decades, the pest has expanded its range to affect all major European and American fruit production regions. The SWD is a highly adaptive insect that is able to disperse, survive, and flourish under a range of environmental conditions. **Figure:1.1**, **Figure:1.2** show how fast this pest has spread in just a few years (from 2015 until 2023).

Infestation by SWD generates both direct and indirect economic impacts through yield losses, the shorter shelf life of infested fruit, and increased production costs. The pest has impacted fresh markets, frozen berries, and fruit export programs due to zero tolerance for fruit infestation [7]. As the SWD control programs rely heavily on insecticides, exceeding the maximum residue levels (MRLs) has also resulted in crop rejections. The economic impact of SWD has been particularly severe for organic operations, mainly due to the limited availability of effective insecticides [8].

³<https://www6.paca.inrae.fr/institut-sophia-agrobiotech>

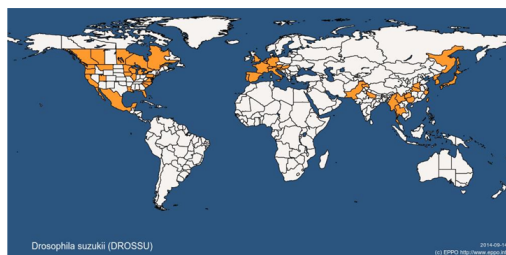


Figure 1.1: Spread of *D. suzukii* worldwide in the 09-02-2015 (source: EPPO Global Database⁴.)

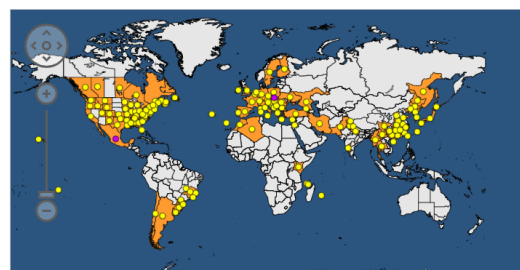


Figure 1.2: Spread of *D. suzukii* worldwide Last updated: 22-05-2023 (source: EPPO Global Database)

Drosophila Suzukii has a high thermal tolerance and a high potential for colonizing different habitats; it is able to withstand both hot summers in Spain and cold areas, such as mountainous regions in Japan and the Alps. Its occurrence was confirmed in mountainous regions by Tonina et al.^{[9][10]}, and its survival in regions with mean daily temperatures below 11°C shows both its adaptive capacity to cold conditions and its tolerance to the wide temperature range typical of mountains.

1.3 The Sterile Insect Technique (SIT)

The idea of the Sterile Insect Technique (SIT) originated in the 1930s and 1940s, credited to three researchers from the USSR, Tanzania, and the USA, for more in-depth information about the historical background of SIT, refer to^[11]. The SIT is a biologically-based method used to control insect pests, particularly those that damage crops (*D. Suzukii*) or spread diseases (e.g. the mosquito *Aedes aegypti*)^[12]. This method involves the mass-rearing of a target insect species, sterilizing them through radiation or other means, and then releasing them into the wild (see figure 1.3). These sterile insects mate with wild counterparts^[13], The huge number of sterile insects released compared to wild ones increases the probability of sterile-wild mating, leading to the production of non-viable eggs or offspring with reduced fitness (sterile offspring or unable to mate)^[14], thereby reducing the pest population over time. If the release is sufficient and the duration of the treatment sufficiently long, it would be possible to eradicate the pests.

The SIT has several advantages compared to other pest management methods, namely the minimization of the environmental impact by reducing chemical contamination due to the overuse of pesticides, and harm to non-target organisms. The technique in some cases, see examples below, enables sustainable control by continuously suppressing eventually the eradication of the pest populations, leading to long-term control and cost savings compared to methods that require frequent pesticide applications. However, such a thing can only be applicable in certain cases. Moreover. The SIT lowers the likelihood of resistance development, making it valuable in integrated pest management strategies. To make the SIT more effective it can be integrated with other pest control methods to enhance its effectiveness.

Though initial setup costs of SIT may be high, the potential for sustained pest control and reduced reliance on chemical pesticides result in long-term economic benefits, particularly in large-scale agricultural systems.

Throughout SIT, the tsetse fly was eradicated from Zanzibar in 1998⁵, and Senegal in 2014⁶, the sweet potato weevil (*Cylas formicarius*) was eradicated from Kume Island and Tsuken Island^[15],

⁴<https://gd.eppo.int/taxon/DROSSU/distribution>

Okinawa Japan^[16].

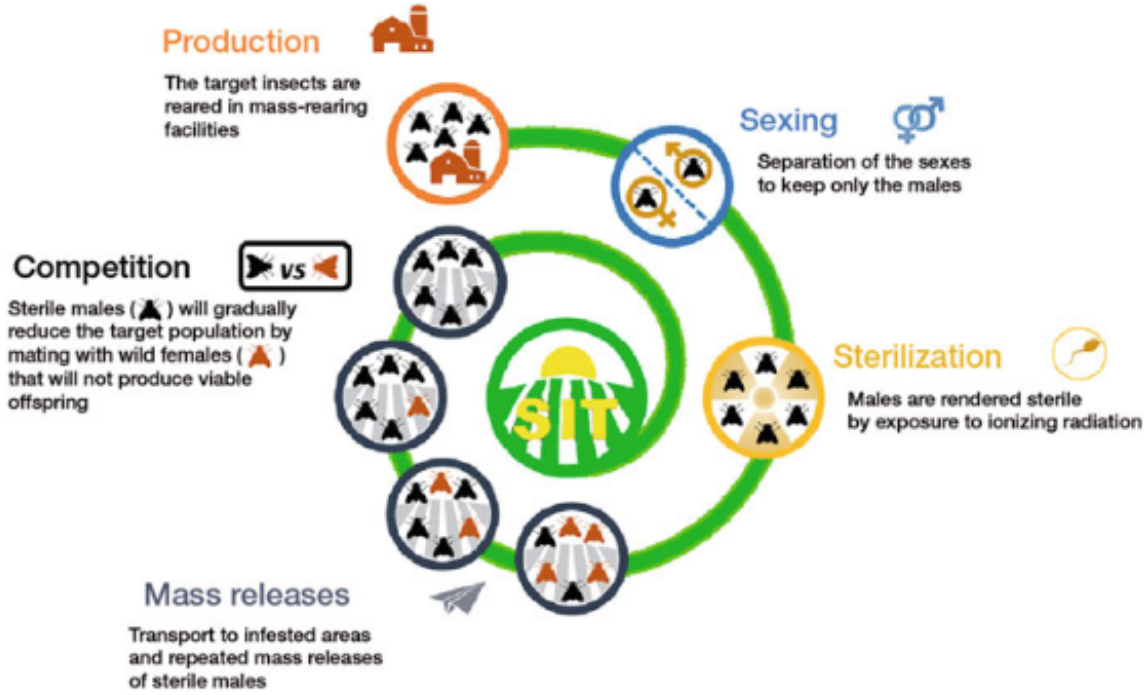


Figure 1.3: Diagram of the main steps of the sterile insect technique^[1]

1.4 The aim of the internship

Traditionally, the Sterile Insect Technique (SIT) primarily focused on the release of sterilized males to disrupt the reproduction of target pests, the main reason is that the male mosquitoes are generally harmless as they do not bite or feed on blood (*Aedes aegypti*) or lay eggs *D.suzukii*. By releasing sterile male mosquitoes into the environment, it is possible to reduce the population of the species without increasing the biting activity in human populations or destroying the harvest, another species where it is relatively easy to determine the sex of insects, such as the Mediterranean fruit fly (*Ceratitidis capitata*)^[17]. However, in the case of *D. suzukii*, technicians spend so much time in the sexing process. Therefore, it becomes important to evaluate the impact and effectiveness of SIT when both sterile males and females are released.

The central objective of this study is constructing an Ordinary Differential Equation (ODE) model to capture the dynamics of *D. suzukii* population incorporating both sterile females and males into the release strategy and comparing its effectiveness to the male-only release. This modeling approach has known a step-by-step reasoning starting with a basic model and adding hypotheses and dimensions in order to find the final model that contains all the hypotheses needed including remating ability, preferences, and many other hypotheses related to fly biology.

The following chapter of this work will highlight, analyze, and simulate the population's dynamics. The chapter will delve into the details of modeling the population dynamics of *Drosophila Suzukii*. It will focus on the theoretical framework and the formulation of the Ordinary Differential Equations (ODEs) used to model the population dynamics of *Drosophila Suzukii* without releasing sterile flies. The modeling aspect will start with a model with three cohorts, analyze it, and simulate it.

⁶Source: UN FAO (Food and Agriculture Organization of the United Nations)

⁶source "The Tsetse Fly Eradication Project in Senegal Wins Award for Best Sustainable Development Practices", International Atomic Energy Agency (IAEA)

Some complexity will be added by adding other compartments that describe the dynamics of the population more broadly with a remating ability for female flies.

In Chapter 3, the same approach will be taken by presenting the same models with the introduction of sterile flies into the population, The chapter is going to be divided into two sections the first one deals with the release of only males, and the second one deals with both males and females. The analyses and simulations are conducted to explore the impact of the different strategies on overall population growth and reproductive success.

The Last chapter summarizes the findings and draws conclusions, it will offer an insight into the efficacy of the Sterile Insect Technique (SIT) approach for controlling this pest species, and at the end, it will highlight the best strategy of release that could help in designing more effective and targeted pest management strategies will be highlighted.

This research represents an exciting advancement in the field, offering valuable insights into the application of the SIT technique for controlling *Drosophila Suzukii*.

Mathematical Modeling of *Drosophila Suzukii*'s population

Mathematical modeling has proved its effectiveness in understanding and predicting the dynamics of the populations and the evaluation of many strategies.. When it comes to the Sterile Insect Technique, mathematical models provide tools for analyzing, simulating, and optimizing the deployment of sterile insects to suppress pest populations.

Mathematical models of population dynamics for SIT usually contain parameters such as population growth rates, mortality rates, mating probabilities, dispersal rates, and the sterilization rate of released insects. By combining these parameters and their interactions in the modeling aspect, these models provide a view of the capability of SIT and assist in optimizing the technique for maximum efficiency

SIT models can be broadly classified into two approaches, discrete-time models, in which changes in population occur at discrete time intervals. In fact, one of the first SIT models was a discrete-time model developed by Edward F. Knipling in the late 1950s and since then modeling has known so much development, and continuous-time models, well-suited for studying population dynamics over continuous time intervals, in this case, continuous mathematical models of the SIT can be based on various mathematical frameworks, including **ordinary differential equations (ODEs)**, and **partial differential equations (PDEs)** ^{[18] [19]}, there are other frameworks such as **Fractional Differential Equations (FDEs)**, and **Stochastic Differential Equations (SDEs)** but ODEs and PDEs are the most applied ones, each modeling approach offers different advantages and is selected based on the specific characteristics of the target species, available data, and research objectives. For the case of *D.suzukii* continuous-time modeling best represents the dynamics of this pest species in the natural environment. This preference arises from processes that govern the behavior of continuous mating and not seasonal mating, growth, lifecycles, and activities of this pest species.

In the modeling aspect of this work, ODEs have been used. ODEs describe the changes in population sizes over time, in the mathematical framework, they are models in finite-dimensional case (i.e. the variables are functions that depend on one variable "time") assuming a well-mixed population. Their value becomes even more evident when we possess limited data about individual insect behaviors. They allow us to express our hypotheses within the model itself, and see its effect on the population dynamic.

Interestingly enough, there are very few contributions to the modeling of *D.Suzukii*'s dynamics in general and even fewer to the application of sterile insect technique on this species. In the literature, we find a study on the modeling of male *D. Suzukii*'s populations using PDEs, this model is based on a physiological approach and substantiated by capture data;^[20] this model is an application of a more general model taken from the article^[21].

This initial chapter addresses the modeling of *D. suzukii* population without release. We base our first ODE on a mating disruption pest control model^[22]. Beginning with a basic three-compartment model, we progressively introduce and analyze additional hypotheses to understand their effects on population dynamics and enhance our calculation skills.

The analysis of the different models is based on several mathematical techniques and concepts. In the following, we outline some key elements involved in the analysis of ODEs:

- 1) Existence and uniqueness of the solution
- 2) Equilibrium Points and their Stability
- 3) Numerical simulations

2.1 First Basic Model of *D. suzukii's* population (3 compartments)

The literature^[7], and^[8] about the biology of *D.suzukii* has enabled us to identify three main stages: the larval stage (L), which groups together the immature stages: eggs, larvae, and pupae; the adult male (M) and female stages. The diagram and the model 2.1 was inspired by the work of Dufour et al^[22]

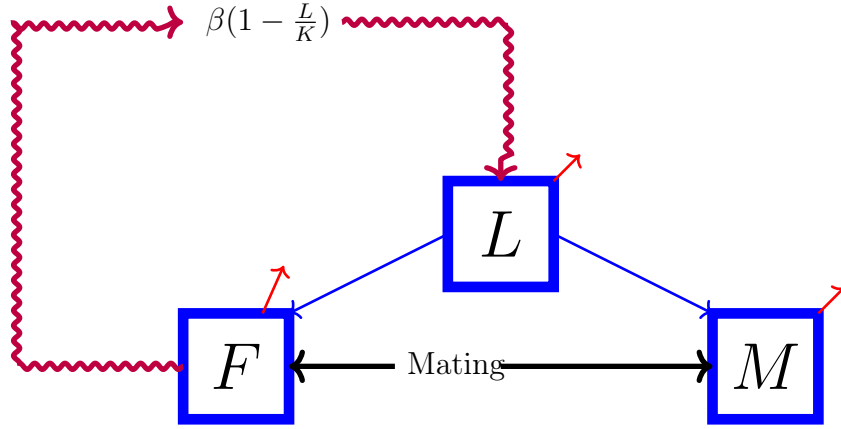


Figure 2.1: Diagram of the population model for TIS *Drosophila suzukii*, corresponding to the system of equations 2.1.

System 2.1 will be called the 3-compartment model, it serves as our starting point, offering a concise representation characterized by fewer dimensions. The dynamics of the population structure in this way are described in Figure:2.1 and by the following system of equations:

$$\begin{cases} \frac{dL}{dt} = \beta \left(1 - \frac{L}{K}\right) \min\left(\frac{\gamma M}{F}, 1\right) v_F F - (v_L + \mu_L) L \\ \frac{dM}{dt} = v_L m L - \mu_M M \\ \frac{dF}{dt} = v_L (1 - m) L - \mu_F F \end{cases} \quad (2.1)$$

Overall, the system of equations represents a model of interactions between males and females (F and M) with a limited carrying capacity on the juvenile population (K).

Let's break down the individual equations and their meanings:

- The first equation represents the population dynamics of Larvae. The rate of change is determined by several factors:
 - The growth rate parameter β : it governs the intrinsic growth potential of the population,
 - The carrying capacity K : represents the maximum population size that the environment can sustain,
 - The term $\left(1 - \frac{L}{K}\right)$: accounts for the limiting effect of population density on growth, it also ensures that the growth of Larvae is limited by the carrying capacity K .

- The term $\min\left(\frac{\gamma^M}{F}, 1\right)$: describes the proportion of population that could mate, and v_F is the mating rate
- The terms $(v_L + \mu_L)$ account for the loss of individuals from the population due to various factors, such as mortality (μ_L) and transformation into adult (v_L).
- The second equation represents the dynamics of the male population M , and it is influenced by:
 - The maturation rate v_L , the number of Larvae that are males is mL , and the parameter m represents the proportion of L that contributes to the growth of M .
 - The term μ_M : represents the mortality rate of adults male.
- The third equation describes the dynamics of the female population F . This equation accounts for the dynamics of the females, which are affected by:
 - The maturation rate v_L that has the same role as the male compartment with $(1 - m)$ as the proportion of females
 - The term μ_F : represents the mortality rate of the female population.

Before starting with analyzing the different models we have to ensure the existence and unicity of the solution

Existence and unicity of the solution

The first model 2.1, and all the models that follow can be written as autonomous dynamical systems of the form:

$$\dot{X} = f(X) \tag{2.2}$$

(2.2) associated with initial condition $X(0) = X_0$ called **"Initial Value Problem" (IVP)** or Cauchy problem.

All that changes in this model and the following models is the explicit writing of $f(X)$ and the size of the state vector X , while in the case of 2.1, it can be written as

$$f(X) = \begin{pmatrix} \beta \left(1 - \frac{L}{K}\right) v_F \min\left(\frac{\gamma^M}{V}, 1\right) F - (\mu_L + v_L) L \\ v_L(1 - m)L - \mu_F F \\ v_L mL - \mu_M M \end{pmatrix} \tag{2.3}$$

with $X = \begin{pmatrix} L \\ F \\ M \end{pmatrix}$

To ensure the existence and unicity of the solution of the IVP, we have the following **Theorem of (Picard-Lindelöf)** [23]

Theorem 2.1.1: (Picard-Lindelöf)

Suppose $f \in C(U, \mathbb{R}^n)$, where U is an open subset of \mathbb{R}^{n+1} , and $(t_0, x_0) \in U$. If f is locally Lipschitz continuous in the second argument, uniformly concerning the first, then there exists a unique local solution $\bar{x}(t) \in C^1(I)$ of the IVP 2.2, where I is some interval around t_0 .

$f(X)$, in this case, 2.1, and in all the cases that follow, is locally Lipschitz continuous with respect to X , and uniformly with respect to t , and thus we can easily prove, following **Theorem: 2.1.1** the existence and the unicity of a **local solution**. A **local solution** refers to a solution of an IVP that exists and is unique only for a limited interval of time, not necessarily covering the entire possible interval of existence.

As a result, we are intrigued to explore the existence of the largest interval where a unique solution to the IVP exists. This exceptional solution is referred to as the "**maximal solution**". The following theorem establishes both the existence and uniqueness of the **maximal solution** for an IVP in the form described by equation 2.2.

Theorem 2.1.2: [23]

Suppose the IVP 2.2 has a unique local solution (e.g. the conditions of Theorem 2.1.1 are satisfied). Then there exists a unique maximal solution defined on some maximal interval $I_{(t_0, x_0)} = (T_-(t_0, x_0), T_+(t_0, x_0))$.

In our case 2.2, since $f(X)$ satisfies theorem 2.1.1 hypothesis, we have a unique maximal solution defined on a certain interval.

As previously mentioned, the solution discovered in the previous theorem is referred to as a maximal solution. A solution that exists for all $t \in \mathbb{R}^+$ is termed a **global solution**, and it's noteworthy that every global solution is also maximal. This leads to the following Corollaries aimed at ensuring global existence:

Corollary 2.1.1: [23]

Let $\phi(t)$ be a solution of 2.2 defined on the interval (t_-, t_+) . Suppose there is a compact set $[t_0, t_+] \times C \subset U$ such that $\phi(t_m) \in C$ for some sequence $t_m \in [t_0, t_+)$ converging to t_+ . Then there exists an extension to the interval $(t_-, t_+ + \varepsilon)$ for some $\varepsilon > 0$.

to understand this result, the logical negation of this Corollary is very interesting.

Corollary 2.1.2

Let $I_{(t_0, x_0)} = (T_-(t_0, x_0), T_+(t_0, x_0))$ be the maximal interval of existence of a solution starting at $x(t_0) = x_0$. If $T_+ = T_+(t_0, x_0) < \infty$, **then the solution must eventually leave every compact set** C with $[t_0, T_+] \times C \subset U$ as it approaches T_+ . In particular, if $U = \mathbb{R} \times \mathbb{R}^n$, the solution must tend to infinity as t approaches T_+ .

Therefore, as all solutions remain confined within a compact set, the inference is that our solution is global.

Conclusion:

We have the following results for all the models that we are working with,

- 1) The solution exists and it is unique
- 2) The solution is global

We will now proceed with an examination of model 2.1. To facilitate this analysis, we will initially assume $\gamma = 1$, signifying that both males and females can mate only once during their lifetimes. Given the presence of the term $\min(\frac{M}{F}, 1)$, we can establish two distinct sub-models based on the relative quantities of females and males.

2.1.1 Male abundance $M \geq F$

The abundance of males will give us $\min(\frac{M}{F}, 1) = 1$ and thus the system 2.1 becomes

$$\begin{cases} \dot{L} = \beta \left(1 - \frac{L}{K}\right) v_F F - (\mu_L + v_L) L \\ \dot{M} = v_L m L - \mu_M M \\ \dot{F} = v_L (1 - m) L - \mu_F F \end{cases} \quad (2.4)$$

Equilibrium points

$$\begin{aligned} \begin{cases} \dot{L} = 0 \\ \dot{M} = 0 \\ \dot{F} = 0 \end{cases} &\implies \begin{cases} \beta \left(1 - \frac{L}{K}\right) v_F F - (\mu_L + v_L) L = 0 \\ v_L m L - \mu_M M = 0 \\ v_L (1 - m) L - \mu_F F = 0 \end{cases} \\ &\implies \begin{cases} L^* = K \left(1 - \frac{1}{\eta_{0M}}\right) \\ M^* = \frac{v_L m}{\mu_M} L^* \\ F^* = \frac{v_L (1 - m)}{\mu_F} L^* \end{cases} \end{aligned}$$

with $\eta_{0M} = \frac{\beta(1-m)v_F v_L}{(\mu_L + v_L)\mu_F}$ as the basic reproduction number or the basic offspring number, the number is a fundamental concept in epidemiology and population biology that measures the potential for disease spread or population growth. In this context, it represents the average number of adult females that can be produced from a single fertilized female during her lifetime. The number contains the average number of adult females $\left(\frac{v_L(1-m)}{(\mu_L + v_L)}\right)$ that we can expect to see emerge from the egg laying rate (β) of a fertilized female $\left(\frac{v_F}{(\mu_F + v_F)}\right)$ during her lifetime $\left(\frac{1}{\mu_F}\right)$.

and thus we have two equilibrium points $E^* = (0, 0, 0)$ and $EE^* = (L^*, F^*, M^*)$:

- if $\eta_{0M} \leq 1$, E^* is the only non negative equilibrium point
- if $\eta_{0M} > 1$ we have the two equilibrium points $E^* = (0, 0, 0)$, and $EE^* = (L^*, F^*, M^*)$ which is positive

Stability of these Equilibrium points

For stability analysis, we employ two methods, which are not interchangeable but rather complement each other. While the first method deduces the local stability of the critical point, the second method helps to determine global stability by using the results obtained from the first method's analysis of local stability.

First method

The following method is based on using the Jacobian matrix to find the eigenvalues and deduce the stability, and in that case, we have the following theorem

Theorem 2.1.3

An equilibrium point \mathbf{X}^* of the ODE is **locally asymptotically stable** if all the eigenvalues of \mathbf{J} , the Jacobian evaluated at \mathbf{X}^* , have negative real parts. The equilibrium point is unstable if at least one of the eigenvalues has a positive real part. However, if some eigenvalues have zero real parts, and others have negative real parts, further analysis is needed.

The Jacobian associated with the system:

$$J = \begin{pmatrix} -(\mu_L + v_L) - v_F \frac{\beta F^*}{K} & v_F \beta \left(1 - \frac{L^*}{K}\right) & 0 \\ v_L(1 - m) & -\mu_F & 0 \\ v_L m & 0 & -\mu_M \end{pmatrix}$$

for $E^* = (0, 0, 0)$ the Jacobian becomes

$$J(E^*) = \begin{pmatrix} -(\mu_L + v_L) & v_F \beta & 0 \\ v_L(1 - m) & -\mu_F & 0 \\ v_L m & 0 & -\mu_M \end{pmatrix}$$

To apply 2.1.1 we will divide the Jacobian matrix into two block matrices, the first one is $A = \begin{pmatrix} -(\mu_L + v_L) & \beta v_F \\ v_L(1 - m) & -\mu_F \end{pmatrix}$ And the second one is $B = (-\mu_F)$ and we will study the eigenvalues of each of these matrices Matrix B has only one negative eigenvalue ($\mu_M > 0$), while for matrix A the trace is negative and the determinant is positive $\iff \eta_{0M} < 1$

for the second equilibrium point $EE^* = (L^*, F^*, M^*)$ the associated Jacobian is

$$J(EE^*) = \begin{pmatrix} -(\mu_L + v_L) - \frac{\beta v_F v_L (1-m)}{\mu_F} \left(1 - \frac{1}{\eta_{0M}}\right) & \frac{v_F \beta}{\eta_{0M}} & 0 \\ v_L(1 - m) & -\mu_F & 0 \\ v_L m & 0 & -\mu_M \end{pmatrix}$$

we will follow the same logic but the change will be in the first matrix $A = \begin{pmatrix} -(\mu_L + v_L) - \frac{\beta v_F v_L (1-m)}{\mu_F} \left(1 - \frac{1}{\eta_{0M}}\right) & \frac{v_F \beta}{\eta_{0M}} \\ v_L(1 - m) & -\mu_F \end{pmatrix}$ and the second one is $B = (-\mu_M)$ we will study the eigenvalues of each of these matrices, the second matrix B has only one negative eigenvalue, for the first matrix A the trace is negative, and

$$\det(A) = \mu_F (\mu_L + v_L) + \beta v_F v_L (1 - m) \left(1 - \frac{1}{\eta_{0M}}\right) - \frac{v_F \beta}{\eta_{0M}} v_L (1 - m) = 1 + \eta_{0M} \left(1 - \frac{1}{\eta_{0M}}\right) - 1 = \eta_{0M} - 1$$

then the stability of $EE^* \iff \det(A) > 0 \iff \eta_{0M} > 1$.

Conclusion:

- if $\eta_{0M} \leq 1$, E^* is the only non-negative equilibrium point and it is LAS
- if $\eta_{0M} > 1$ we have two equilibrium points $E^* = (0, 0, 0)$, and $EE^* = (L^*, F^*, M^*)$ which is positive, E^* is unstable, and EE^* LAS

Second Method

The analysis of the system 2.4 uses the theory of cooperative systems [24]

Let an autonomous system of ODEs

$$\frac{dx}{dt} = \Psi(x) \quad (2.5)$$

where $\Psi : D \rightarrow \mathbb{R}^n, x \in D \subset \mathbb{R}^n$, is called cooperative if Ψ_i is monotone increasing with respect to $x_j, \forall i, j \in [1, \dots, n], j \neq i$. A function Ψ with the stated monotonicity is called a quasi-monotone.

Theorem 2.1.4: [24] Theorem 3.1, p. 18]

Let $a, b \in D$, such that $a \leq b, [a, b] \subseteq D$ and $f(b) \leq \mathbf{0} \leq f(a)$. Then 2.5 defines a positive dynamical system on $[a, b]$. Moreover, if $[a, b]$ contains a unique equilibrium p then, p is globally asymptotically stable (GAS) on $[a, b]$.

Theorem 2.1.5: [25] Theorem 6

Let $a, b \in D$, such that $a \leq b, [a, b] \subseteq D$ and $f(a) = f(b) = 0$ for 2.5. Then
 (a) 2.5 defines a positive dynamical system on $[a, b]$.
 (b) If a and b are the only equilibrium of the dynamical system on $[a, b]$, then all solutions initiated in the interior of $[a, b]$ converge to one of them, that is, either all converge to a or all converge to b .

Stability Proof the second method is based on the two theorems 2.1.4 and 2.1.5

We will first apply theorem 2.1.4 we take $a = (0, 0, 0)$ and we will construct b such that the hypothesis in theorem 2.1.4 is fulfilled.

we have then $f(a) = 0$ and for $b = y_q$ such that $q \geq K$ and $y_q = \begin{pmatrix} K \\ \frac{v_L m}{\mu_M} q \\ \frac{v_L(1-m)}{\mu_F} q \end{pmatrix}$ we get $f(y_q) \leq 0$

then we have a positive dynamical system on $[0, y_q]$.

Let $\eta_{0M} \leq 1$, in this case, E^* is the only equilibrium on $[0, y_q]$ and it follows from 2.1.5 that it is GAS on $[0, y_q]$. Hence, E^* is also GAS on $\cup_{q \geq K} [0, y_q] = \Omega_K = \{x \in \mathbb{R}_+^3 : L \leq K\}$.

Let $\eta_{0M} > 1$. First, using the same approach, theorem 2.1.4, we obtain that EE^* is GAS on $\{x \in \mathbb{R}_+^3 : x \geq EE^*\}$. Second, we are left with the interval $[E^*, EE^*]$. Following the results in method 1, for $\eta_{0M} > 1$ the equilibrium E^* is not stable, thus the theorem 2.1.5 implies that EE^* attracts all solutions in the interior of the interval. Putting the two results together we obtain that EE^* is GAS on the interior of \mathbb{R}_+^3 . The asymptotic behavior of the solutions on the boundary of \mathbb{R}_+^3 can be verified directly to obtain the GAS property of EE^* .

Conclusion:

- Let $\eta_{0M} \leq 1$, then E^* is the only equilibrium and it is GAS
- Let $\eta_{0M} > 1$. we have two equilibrium points E^* , and EE^* , while the positive critical point is the only GAS

2.1.2 Male scarcity $M < F$

In this case $\min(\frac{M}{F}, 1) = \frac{M}{F}$, and our model can be written as

$$\begin{cases} \dot{L} = \beta \left(1 - \frac{L}{K}\right) v_F M - (\mu_L + v_L) L \\ \dot{M} = v_L m L - \mu_M M \\ \dot{F} = v_L (1 - m) L - \mu_F F \end{cases} \quad (2.6)$$

Equilibrium points

$$\begin{cases} \dot{L} = 0 \\ \dot{M} = 0 \\ \dot{F} = 0 \end{cases} \implies \begin{cases} \beta \left(1 - \frac{L}{K}\right) v_F M - (\mu_L + v_L) L = 0 \\ v_L m L - \mu_M M = 0 \\ v_L (1 - m) L - \mu_F F = 0 \end{cases}$$

$$\implies \begin{cases} L^* = K \left(1 - \frac{1}{\eta_{0F}}\right) \\ M^* = \frac{v_L m}{\mu_M} L^* \\ F^* = \frac{v_L (1 - m)}{\mu_F} L^* \end{cases}$$

$\eta_{0F} = \frac{\beta m v_F v_L}{(\mu_L + v_L) \mu_M}$ as the basic reproduction number or the basic offspring number in the male scarcity case. the only difference between this offspring number and the previous one is the focus of the number, in the previous one we focused on the females and now we re focusing on the males. It represents the average number of adult males that can be produced by a single male during his lifetime

As we can see we have two equilibrium points $E^* = (0, 0, 0)$ and $EE^* = (L^*, M^*, F^*)$ while $E^* = (0, 0, 0)$ is the only equilibrium point if $\eta_{0F} \leq 1$

Stability analysis

The Jacobian associated with the system:

$$J = \begin{pmatrix} -(\mu_L + v_L) - \frac{v_F \beta M^*}{K} & v_F \beta \left(1 - \frac{L^*}{K}\right) & 0 \\ v_L m & -\mu_M & 0 \\ v_L (1 - m) & 0 & -\mu_F \end{pmatrix}$$

We can notice that this Jacobian matrix is the same as the Jacobian matrix already analyzed in the male abundance area but with a small rearrangement of females and males compartment in the model 2.6 and therefore following the same proof we can deduce that

Conclusion 1:

- if $\eta_{0F} \leq 1$, then E^* is the only equilibrium and it is GAS
- if $\eta_{0F} > 1$. we have two equilibrium points E^* and EE^* , while E^* is unstable, we have that EE^* the strictly positive critical point is GAS

conclusion 2:

We suppose that η_{0F} is the male's scarcity basic offspring number and η_{0M} is the male's abundancy then we have:

- if $\mu_M > \mu_F$ we have that $\frac{\eta_{0F}}{\eta_{0M}} = \frac{\frac{\beta m v_L}{(\mu_L + v_L)\mu_M}}{\frac{\beta(1-m)v_L}{(\mu_L + v_L)\mu_F}} = \frac{m\mu_F}{(1-m)\mu_M}$ in the *D. suzukii* case $m = (1 - m)$ then we obtain $\eta_{0F} < \eta_{0M}$ which can be described as the reproduction number in the male scarcity area is less than its counterpart in the abundance area, in that case, with $\mu_M > \mu_F$ and $\eta_{0M} > \eta_{0F} > 1$ the equilibrium points of the male scarcity and male abundance fulfill $M^* < F^*$, Therefore, we can conclude that regardless of the system's initial conditions, the dynamics of the system 2.1 will always lead to a state of male scarcity.
- Now if $\mu_M < \mu_F$ we have then $\frac{\eta_{0F}}{\eta_{0M}} = \frac{\frac{\beta m v_L}{(\mu_L + v_L)\mu_M}}{\frac{\beta(1-m)v_L}{(\mu_L + v_L)\mu_F}} = \frac{m\mu_F}{(1-m)\mu_M}$ in the *D. Suzukii* case $m = (1 - m)$ then we obtain $\eta_{0F} > \eta_{0M}$ which can be described as the reproduction number in the males abundance area is greater than its counterpart in the scarcity area, in that case, with $\mu_M < \mu_F$ and $\eta_{0M} > 1$ we have that the equilibrium points of the male scarcity and male abundance fulfill $M^* > F^*$. Therefore, we can conclude that regardless of the system's initial conditions, the dynamics of the system 2.1 will always lead to a state of male abundance.

Simulation

To simulate and illustrate our findings, we need data that have all parameters within the system described by equation 2.1. Our literature search has yielded two datasets, differing due to the variable development of *D. suzukii*, influenced by factors such as abiotic, biotic, and likely genetic elements. This diversity necessitates dual-dataset analysis, and it will help us to verify many results we already mentioned.

The data detailed in table 3.1 are a combination of field and laboratory data on *D. Suzukii* biology and population dynamics. The first dataset in table 3.1, is taken from references [26], [27], and [28]. The second dataset, found in the same table, is extracted from [29].

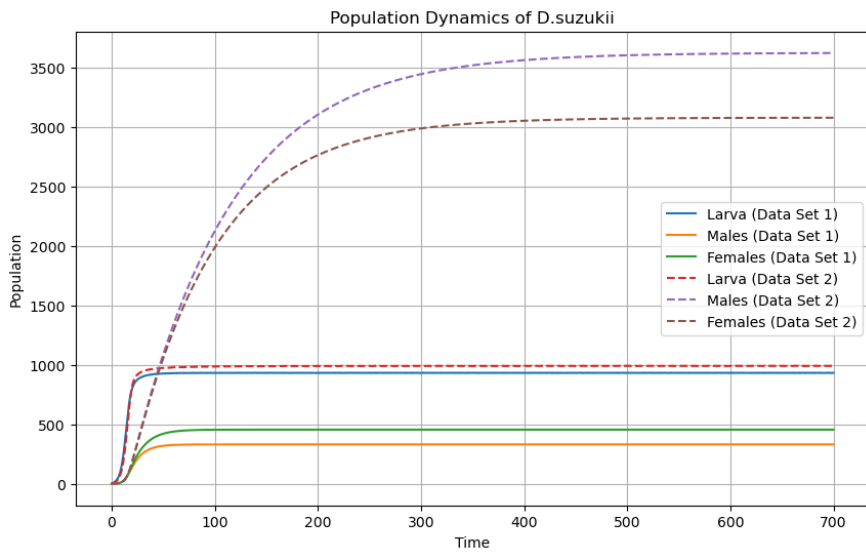


Figure 2.2: Simulation of *Drosophila suzukii* population evolution, with $L = 0$, $M = 1$ and $F = 1$ as an initial condition for both sets of Data

Figure 2.2 illustrates the simulation of system equation 2.1, where initial values were set as $M = 1$ and $F = 1$ to highlight the rapid evolutionary dynamics of the *Drosophila suzukii* population originating from a single pair. The contrast in mortality rates between the first and second datasets, whether affecting males or females, explains the population growth disparity. This discrepancy underscores why the population count in the second dataset evolves at a notably higher rate than that in the first dataset in figure 2.2.

Since we are analyzing the dynamics of system 2.1, we could potentially encounter two submodels: one linked to system 2.4, emphasizing male abundance, and another related to system 2.6, focusing on male scarcity. In either scenario, given that $\eta_{0M} > 1$ and $\eta_{0F} > 1$ in both sets of data, the second equilibrium point $EE^* > (0, 0, 0)$ exhibits Globally Asymptotically Stability (GAS), as depicted in Figure 2.2.

from figure 2.2, and 2.3 the impact of the mortality rates μ_M and μ_F on the population while starting from the same number of population for males and females can be seen in figures 2.3. In the initial dataset, we observe $\mu_M > \mu_F$, then the population will be in the male scarcity while within the second dataset, the population will be in the male abundance area.

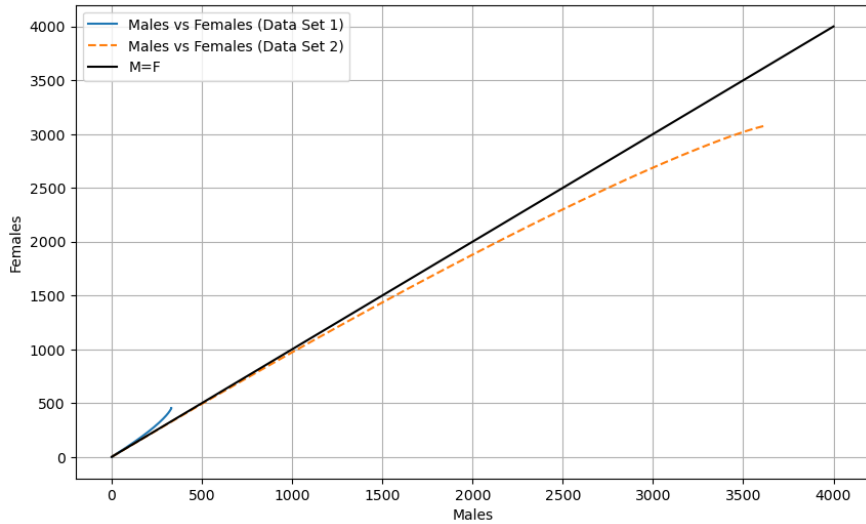


Figure 2.3: Gender Balance of *D. suzukii*: Males vs Females Numbers in the case of the 2.1

2.2 Second Model (4 compartments) Incorporating Conditional Mating Abilities for Males and Females

In the following model, we introduce additional complexity to model 2.1. This complexity arises from differentiating between two types of females: those denoted as V females, which are ready to mate and don't lay eggs, and F females, which have successfully bred and are ready to lay eggs. The introduction of these distinct compartments allows the F females to return to the virgin compartment V , granting them the ability to re-mate. This ability is governed by the proportion δ , which determines the transfer rate to the V compartment for previously mated females.

The compartment V now represents two groups of females: those who have never mated and those who are prepared to mate again after having already bred and produced offspring. As a consequence, females in the F compartment of this model can produce offspring independently, without the need for male mating. This implies that they are fertile even in the absence of males, as mating now occurs in the V compartment.

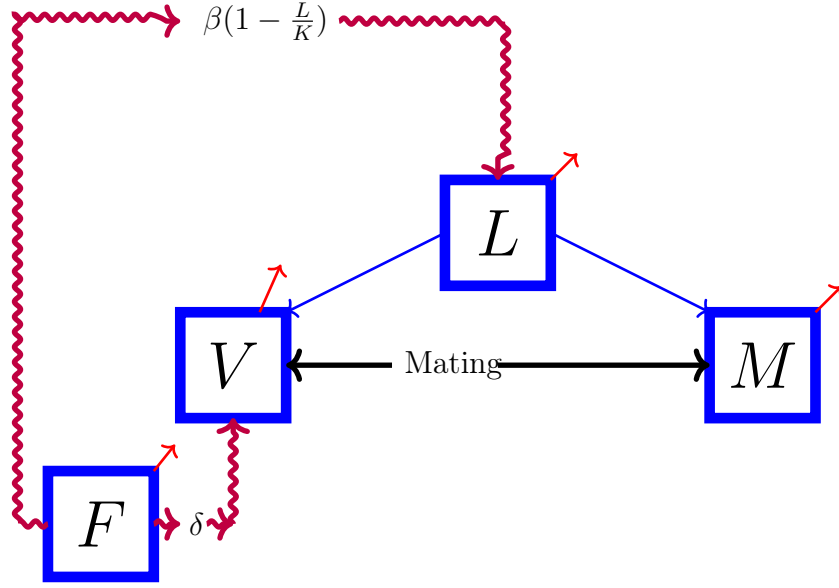


Figure 2.4: Diagram of the population model of *Drosophila suzukii*, corresponding to the system of equations 2.7

$$\begin{cases} \dot{L} = \beta \left(1 - \frac{L}{K}\right) F - (\mu_L + v_L) L \\ \dot{M} = v_L m L - \mu_M M \\ \dot{V} = v_L (1 - m) L + \delta F - (\mu_F + v_F \min(\frac{\gamma^M}{V}, 1)) V \\ \dot{F} = v_F \min(\frac{\gamma^M}{V}, 1) V - (\mu_F + \delta) F \end{cases} \quad (2.7)$$

as was previously explained this equation can be divided into two other models depending on the value of $\min(\frac{\gamma^M}{V}, 1)$

2.2.1 Male abundance $M\gamma > V$

In this case $\min(\frac{\gamma^M}{V}, 1) = 1$

$$\begin{cases} \dot{L} = \beta \left(1 - \frac{L}{K}\right) F - (\mu_L + v_L) L \\ \dot{M} = v_L m L - \mu_M M \\ \dot{V} = v_L (1 - m) L + \delta F - (\mu_F + v_F) V \\ \dot{F} = v_F V - (\mu_F + \delta) F \end{cases} \quad (2.8)$$

Equilibrium points

$$\begin{cases} \dot{L} = 0 \\ \dot{M} = 0 \\ \dot{V} = 0 \\ \dot{F} = 0 \end{cases} \implies \begin{cases} \beta \left(1 - \frac{L}{K}\right) F - (\mu_L + v_L) L = 0 \\ v_L m L - \mu_M M = 0 \\ v_L (1 - m) L + \delta F - (\mu_F + v_F) V = 0 \\ v_F V - (\mu_F + \delta) F = 0 \end{cases}$$

$$\Rightarrow \begin{cases} \text{The first equation gives } F^* = \frac{(\mu_L + v_L)}{\beta \left(1 - \frac{L^*}{K}\right)} L^* \\ \text{The second equation gives } M^* = \frac{v_L m}{\mu_M} L^* \\ \text{The fourth equation gives } V^* = \frac{(\mu_F + \delta)}{v_F} F^* \end{cases}$$

$$\text{and the third equation gives } \eta_{03} \left(1 - \frac{L^*}{K}\right) = 1,$$

$$\Leftrightarrow L^* = K \left(1 - \frac{1}{\eta_0}\right)$$

with $\eta_0 = \frac{\beta(1-m)v_L v_F}{(\mu_L + v_L)((v_F + \mu_F)(\delta + \mu_F) - \delta v_F)}$ as the basic reproduction number or the basic offspring number,

And thus, the system:

- if $\eta_{03} \leq 1$, the system 2.8 has $E^* = (0, 0, 0, 0)$ as the only point of equilibrium
- if $\eta_0 > 1$, the system 2.8 has a trivial equilibrium point $E^* = (0, 0, 0, 0)$ and a unique endemic equilibrium $EE^* = (L^*, M^*, V^*, F^*)$.

Stability analysis

The Jacobian matrix related to the system is:

$$J = \begin{pmatrix} -(\mu_L + v_L) - \frac{\beta F^*}{K} & 0 & 0 & \beta \left(1 - \frac{L^*}{K}\right) \\ v_L m & -\mu_M & 0 & 0 \\ v_L(1 - m) & 0 & -(\mu_F + v_F) & \delta \\ 0 & 0 & v_F & -(\mu_F + \delta) \end{pmatrix}$$

A Metzler matrix is a matrix in which all off-diagonal elements are non-negative, this property is used to describe cooperative or positive interactions in a system. Many results exist on these matrices, including the following proposition [30].

Proposition 2.2.1: [30]

Let M be a Metzler Matrix that can be written in blocks as follows:

$$M = \begin{pmatrix} A & B \\ C & D \end{pmatrix}$$

M is Metzler stable if and only if A and $D - CA^{-1}B$ are Metzler stable.

- then for $E^* = (0, 0, 0, 0)$

$$J(E^*) = \begin{pmatrix} -(\mu_L + v_L) & 0 & 0 & \beta \\ v_L m & -\mu_M & 0 & 0 \\ v_L(1-m) & 0 & -(\mu_F + v_F) & \delta \\ 0 & 0 & v_F & -(\mu_F + \delta) \end{pmatrix}$$

The Jacobian J evaluated at the trivial equilibrium point $X = (0,0,0,0)$ is a Metzler matrix, subdivision the matrix to better see how we get what we are searching for, we have:

$$J(E^*) = \left(\begin{array}{cc|cc} -(\mu_L + v_L) & 0 & 0 & \beta \\ v_L m & -\mu_M & 0 & 0 \\ \hline v_L(1-m) & 0 & -(\mu_F + v_F) & \delta \\ 0 & 0 & v_F & -(\mu_F + \delta) \end{array} \right)$$

So the decomposition of the Metzler matrix given in **Proposition: 2.2.1** gives:

$$\Lambda_0 = \begin{pmatrix} -(\mu_L + v_L) & 0 \\ v_L m & -\mu_M \end{pmatrix}; B_0 = \begin{pmatrix} 0 & \beta \\ 0 & 0 \end{pmatrix};$$

$$C_0 = \begin{pmatrix} v_L(1-m) & 0 \\ 0 & 0 \end{pmatrix}; D_0 = \begin{pmatrix} -(\mu_F + v_F) & \delta \\ v_F & -\mu_F \end{pmatrix}$$

It is trivial that Λ_0 is Metzler stable. Let's check whether $D_0 - C_0 \Lambda_0^{-1} B_0$ is a stable Metzler matrix.

$$\begin{aligned} D_0 - C_0 \Lambda_0^{-1} B_0 &= \begin{pmatrix} -(\mu_F + v_F) & \delta \\ v_F & -(\mu_F + \delta) \end{pmatrix} - \begin{pmatrix} v_L(1-m) & 0 \\ 0 & 0 \end{pmatrix} \begin{pmatrix} -\frac{1}{\mu_L + v_L} & 0 \\ -\frac{v_L m}{\mu_M(\mu_L + v_L)} & -\frac{1}{\mu_M} \end{pmatrix} \begin{pmatrix} 0 & \beta \\ 0 & 0 \end{pmatrix} \\ &= \begin{pmatrix} -(\mu_F + v_F) & \delta + \frac{\beta v_L(1-m)}{(\mu_L + v_L)} \\ v_F & -(\mu_F + \delta) \end{pmatrix} \end{aligned}$$

$(D_0 - C_0 \Lambda_0^{-1} B_0)$ is Metzler. Let's check its stability. Since the trace of this matrix is negative, the stability condition for $(D_0 - C_0 \Lambda_0^{-1} B_0)$ resides in its determinant if it is positive we have the stability, then:

$$\begin{aligned} \det(D_0 - C_0 \Lambda_0^{-1} B_0) &= (\mu_F + \delta)(\mu_F + v_F) - v_F(\delta + \frac{\beta v_L(1-m)}{(\mu_L + v_L)}) > 0 \iff 1 - \eta_0 > 0 \\ &\iff \eta_0 < 1 \end{aligned}$$

then the stability of E^* is insured by $\eta_0 < 1$

- and for $EE^* = (L^*, M^*, V^*, F^*)$

$$J(EE^*) = \left(\begin{array}{cc|cc} -(\mu_L + v_L) \eta_0 & 0 & 0 & \frac{\beta}{\eta_0} \\ v_L m & -\mu_M & 0 & 0 \\ \hline v_L(1-m) & 0 & -(\mu_F + v_F) & \delta \\ 0 & 0 & v_F & -(\mu_F + \delta) \end{array} \right)$$

The decomposition of $J(EE^*)$ by blocks is as follows:

$$\Lambda_1 = \begin{pmatrix} -\eta_0(\mu_L + v_L) & 0 \\ v_L m & -\mu_M \end{pmatrix}; B_1 = \begin{pmatrix} 0 & \frac{\beta}{\eta_0} \\ 0 & 0 \end{pmatrix}; C_1 = \begin{pmatrix} v_L(1-m) & 0 \\ 0 & 0 \end{pmatrix};$$

and

$$D_1 = \begin{pmatrix} -(\mu_F + v_F) & \delta \\ v_F & -(\mu_F + \delta) \end{pmatrix}$$

Λ_1 is Metzler stable. Let's verify if $D_1 - C_1 \Lambda_1^{-1} B_1$ is Metzler stable.

$$\begin{aligned} D_1 - C_1 \Lambda_1^{-1} B_1 &= \begin{pmatrix} -(\mu_F + v_F) & \delta \\ v_F & -(\mu_F + \delta) \end{pmatrix} - \begin{pmatrix} v_L(1-m) & 0 \\ 0 & 0 \end{pmatrix} \begin{pmatrix} -\frac{1}{\eta_0(\mu_L + v_L)} & 0 \\ -\frac{v_L m}{\mu_M \eta_0(\mu_L + v_L)} & -\frac{1}{\mu_M} \end{pmatrix} \begin{pmatrix} 0 & \frac{\beta}{\eta_0} \\ 0 & 0 \end{pmatrix} \\ &= \begin{pmatrix} -(\mu_F + v_F) & \delta + \frac{\beta v_L(1-m)}{\eta_0^2(\mu_L + v_L)} \\ v_F & -(\mu_F + \delta) \end{pmatrix} \end{aligned}$$

$D_1 - C_1 \Lambda_1^{-1} B_1$ is Metzler, its trace being negative, the stability condition is verified by:

$$(\mu_F + \delta)(\mu_F + v_F) - v_F \left(\delta + \frac{\beta v_L(1-m)}{\eta_0^2(\mu_L + v_L)} \right) > 0 \iff 1 - \frac{\eta_0}{\eta_0^2} > 0$$

$$\iff \eta_0 > 1$$

2.2.2 males scarcity $M\gamma < V$

in this case $\min(\frac{\gamma^M}{V}, 1) = \frac{\gamma^M}{V}$ we got then

$$2.7 \implies \begin{cases} \dot{L} = \beta \left(1 - \frac{L}{K}\right) F - (\mu_L + v_L) L \\ \dot{M} = v_L m L - \mu_M M \\ \dot{V} = v_L(1-m)L + \delta F - V\mu_F - v_F \gamma M \\ \dot{F} = v_F \gamma M - (\mu_F + \delta) F \end{cases} \quad (2.9)$$

Equilibrium points

$$\begin{cases} \dot{L} = 0 \\ \dot{M} = 0 \\ \dot{V} = 0 \\ \dot{F} = 0 \end{cases} \implies \begin{cases} \beta \left(1 - \frac{L}{K}\right) F - (\mu_L + v_L) L = 0 \\ v_L m L - \mu_M M = 0 \\ v_L(1-m)L + \delta F - \mu_F V - v_F \gamma M = 0 \\ v_F \gamma M - (\mu_F + \delta) F = 0 \end{cases}$$

$$\implies \text{the first equation gives } F^* = \frac{(\mu_L + v_L)}{\beta \left(1 - \frac{L}{K}\right)} L^*$$

$$\text{the second one gives } M^* = \frac{v_L m}{\mu_M} L^*$$

we get from the forth equation $F^* = \frac{v_F \gamma}{(\mu_F + v_\delta)} M^* = \frac{v_F \gamma}{(\mu_F + \delta)} \frac{v_L m}{\mu_M} L^* = \frac{(\mu_L + v_L)}{\beta \left(1 - \frac{L^*}{K}\right)} L^*$

lastly from the third equation

$$V^* = \left(\frac{m v_L v_F \gamma}{\mu_M} + \frac{\mu_L + v_L}{\beta} \eta_0 + v_L (1 - m) \right) L^* = \frac{(1 - m) v_L (\delta + \mu_F) \mu_M - v_F \gamma m v_L \mu_F}{\mu_F (\delta + \mu_F) \mu_M} L^*$$

with

$$\eta_{04} = \frac{\beta m \gamma v_L v_F}{\mu_M (\mu_L + v_L) (\delta + \mu_F)}$$

as the basic reproduction number or the basic offspring number,

And thus, the system 2.9 has:

- $E^* = (0, 0, 0, 0)$ as the only point of equilibrium if $\eta_{04} \leq 1$
- a trivial equilibrium point $E^* = (0, 0, 0, 0)$ and a unique endemic equilibrium $EE^* = (L^*, M^*, V^*, F^*)$ if $\eta_{04} > 1$.

Stability analysis

The Jacobian matrix is

$$J = \begin{pmatrix} -(\mu_L + v_L) - \frac{\beta F^*}{K} & 0 & 0 & \beta \left(1 - \frac{L^*}{K}\right) \\ v_L m & -\mu_M & 0 & 0 \\ v_L (1 - m) & -v_F \gamma & -\mu_F & \delta \\ 0 & v_F \gamma & 0 & -(\mu_F + \delta) \end{pmatrix}$$

since V variable doesn't influence any other variable, in that case then we can find the critical points of the only three compartments M, F, and L, and deduce their stability.

and thus its Jacobian matrix becomes

$$J = \begin{pmatrix} -(\mu_L + v_L) - \frac{\beta F^*}{K} & 0 & \beta \left(1 - \frac{L^*}{K}\right) \\ v_L m & -\mu_M & 0 \\ 0 & v_F \gamma & -(\mu_F + \delta) \end{pmatrix}$$

we can notice through J that our model wit just the three compartment L , M , and F represents a cooperative system

To find the stability we will use the two previously mentioned theorems, **Theorem 2.1.4**, and **Theorem 2.1.5**.

Proof. As we have said solving $f(X) = 0$ yields two solutions EE^* and E^* , where $E^* > 0$ is the only equilibrium point if $\eta_{04} < 1$ and we have two equilibrium points E^* and $EE^* > 0$ iff $\eta_{04} > 1$. following the two **Theorem 2.1.4**, and **Theorem 2.1.5** we can

deduce the Global stability of the equilibrium. as we see that our system is cooperative on $\Omega_K = \{x \in \mathbb{R}_+^3 : L \leq K\}$.

Let $q \in \mathbb{R}, q \geq K$. we write q as

$$y_q = \begin{pmatrix} K \\ \frac{v_L m}{\mu_M} q \\ \frac{v_F \gamma}{(\mu_F + v_\delta)} \frac{v_L m}{\mu_M} q \end{pmatrix}$$

We have $f(\mathbf{0}) = \mathbf{0}$ and $f(y_q) \leq \mathbf{0}$. Then, following **Theorem 2.1.4** we obtain that f defines a positive dynamical system on $[0, y_q]$.

Let $\eta_{04} \leq 1$. In this case, E^* is the only equilibrium on $[0, y_q]$ and we deduce from **Theorem 2.1.5** that it is GAS on $[0, y_q]$. Hence, E^* is also GAS on $U_{q \geq K} [0, y_q] = \Omega_K$.

Now let $\eta_{04} > 1$. First, we can notice that for $y_q \geq EE^*$ we can verify that we have $f(EE^*) = 0$ and $f(y_q) \leq 0$ and thus EE^* is GAS on $U_{q \geq K} [EE^*, y_q] = \{x \in \mathbb{R}_+^3 : x \geq EE^*\}$. Secondly, we consider **Theorem 2.1.5** applied to the interval $[E^*, EE^*]$. Since for $\eta_{04} > 1$ the equilibrium E^* is not stable, now we consider it as unstable, I will show that it is not stable at the end of the proof, the theorem implies that EE^* attracts all solutions in the interior of the interval. Putting the two results together we obtain that EE^* is GAS on the interior of $\mathbb{R}_+^3 \setminus \{x \in \mathbb{R}_+^3, L = M = F = 0\}$.

- for the stability analysis of E^* we have

$$J(E^*) = \begin{pmatrix} -(\mu_L + v_L) & 0 & \beta \\ v_L m & -\mu_M & 0 \\ 0 & v_F \gamma & -(\mu_F + \delta) \end{pmatrix}$$

Conclusion 2.2.1

Further, let's assume that, at equilibrium, males are abundant, these assumptions can be written as:

1. $\eta_{03} > 1$, while η_{03} is the male abundancy's basic offspring number and η_{04} is related to the male scarcity part
2. $V^* < \gamma M^*$.

Under assumption (2) we have that $M^* \gamma > V^*$ and thus the inequality

$$\gamma > \frac{(1 - m)(\delta + \mu_F) \mu_M}{m((v_F + \mu_F)(\delta + \mu_F) - \delta v_F)}$$

is equivalent to

$$\frac{\eta_{04}}{\eta_{03}} = \frac{\gamma m((v_F + \mu_F)(\delta + \mu_F) - \delta v_F)}{(1 - m)(\delta + \mu_F) \mu_M} > 1$$

Therefore under assumptions (1) and (2), we have that $\eta_{04} > 1$, and by Theorem previously mentioned, we have that the system 2.9 with the scarcity males has a non-trivial equilibrium EE^* , which is GAS on $\mathbb{R}_+ \times \mathbb{R} \times \mathbb{R}_+^2 \setminus \{(L, V, F, M)^T : L = F = M = 0\}$. Furthermore, under (2), (we take now V^* and M^* related to the system 2.9 males scarcity)

$$V^* - \gamma M^* = L^* \left(\frac{(1 - m)v_L(\delta + \mu_F) \mu_M - v_F \gamma v_L \mu_F}{\mu_F(\delta + \mu_F) \mu_M} - \gamma \frac{mv_L}{\mu_M} \right)$$

$$\begin{aligned}
 &< \frac{v_L L^*}{\mu_M} \left(\frac{m \mu_M}{\mu_F} - \frac{m(\delta + \mu_F) \mu_M}{((v_F + \mu_F)(\delta + \mu_F) - \delta v_F)} \frac{v_F \mu_F + \mu_F(\delta + \mu_F)}{\mu_F(\delta + \mu_F)} \right) \\
 &< \frac{v_L L^*}{\mu_M} \left(\frac{m \mu_M}{\mu_F} - \frac{r \mu_M}{\mu_F} \right) = 0.
 \end{aligned}$$

and also we get that $V^* < \gamma M^*$ which means that the equilibrium points of the system 2.9 are in the male abundance area.

To summarize, under assumptions (1) and (2), the globally asymptotically stable equilibrium EE^* for male scarcity and abundance, respectively, are in the male abundance region defined via $V^* < \gamma M^*$. Therefore, the equilibrium point EE^* , related to the male abundance area, is a regular equilibrium of the whole system under constraint, while EE^* related to the male scarcity is a virtual one. Moreover, we have the following theorem

Theorem 2.2.1

Given (1) and (2), our dynamical system under constraints defines a positive dynamical system on \mathbb{R}_+^4 and has two equilibria in this domain:

- (a) E^* , which is unstable, and
- (b) EE^* , which is GAS on $\mathbb{R}_+^4 \setminus \{(L, V, F, M)^T \in \mathbb{R}_+^4 : L = V = F = 0 \text{ or } L = F = M = 0\}$.

Simulation

In order to illustrate our findings, we will use two simulations. The initial illustration 2.5 depicts the population dynamics along with its associated equilibrium points. Within this visual, both datasets provide confirmation for the hypothesis discussed in conclusion 2.2.2, and thus we end up in the male abundance area, which can be seen in Figure 2.6.

We chose $V = 1$ and $M = 1$ and zero for the other compartments to illustrate the rapid development of the population in such a short time in a new environment.

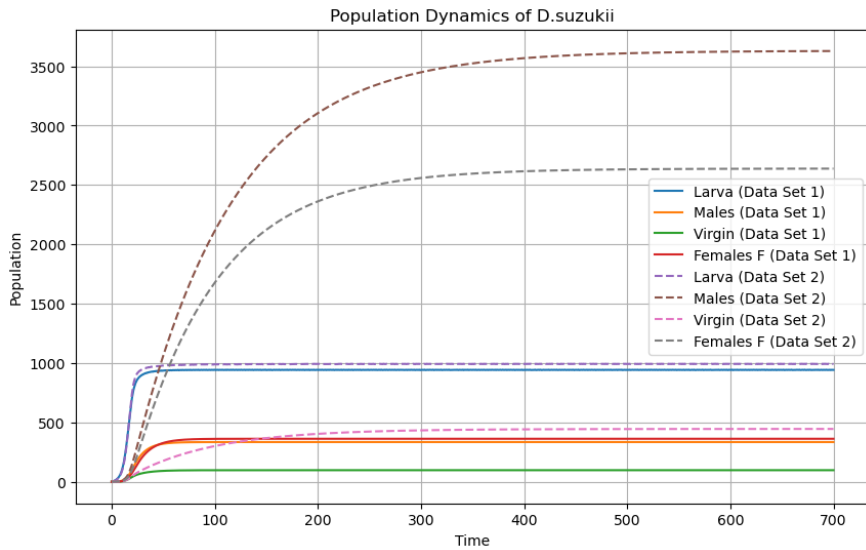


Figure 2.5: Population Dynamics over Time: in the Model 3.1 without Constraints, $L = 0$, $M = 1$, $V = 1$, $F = 0$

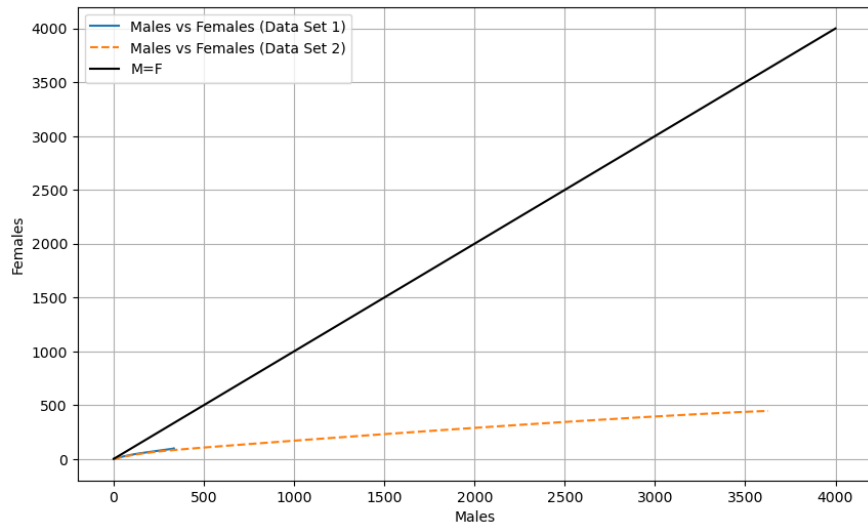


Figure 2.6: Sex ratio of *D. suzukii*: Males vs. Females Numbers in the case of the 3.1 model, starting from $M = 1$, and $F = 1$

Modeling the SIT releases

This chapter focuses on modeling the Sterile Insect Technique (SIT), involving the introduction of sterile individuals to control the pest population. We will systematically incorporate this concept into our models, progressing in a step-wise manner. Initially, we will introduce an additional variable denoted as "sterile males M_s " into the models. We plan to begin with the 3-compartment model 2.6 with three dimensions and gradually introduce hypotheses and increase the dimension. Once the model becomes intricate 3.5, we will delve into numerical analyses.

By comparing systems 2.1 and 2.6, a transformation is evident: the replacement of $\min(\frac{M}{F}, 1)$ with $\frac{M}{M+M_s}$. The alteration essence from two hypotheses. First, in system 2.1 we just need a female to mate to have eggs. Consequently, $\min(\frac{M}{F}, 1)$ simplifies to 1, given the saturation of mating opportunities through released males. Second, the calculation of viable eggs produced by a female now hinges on the probability of mating with wild males, denoted by $\frac{M}{M+M_s}$. This adaptation models the impact of the SIT strategy on mating dynamics. particularly focusing on the significant deployment of sterile males

In the subsequent section, we will extend our approach to encompass "sterile females F_s " in addition to sterile males M_s , following the same systematic progression. It's important to acknowledge that the dynamics of the sterile population are distinct, primarily affecting the mating dynamics of the non-sterile populations. Furthermore, it is assumed that all mated females, regardless of whether it's with sterile or fertile males, exit the virgin females' cohort V , in both systems that incorporate Virgins 3.11, and 3.12, contributing to the fertilized females compartment F only if fertilized by fertile males.

Moreover, the assumption is made that mating occurs randomly among the male population. Consequently, the proportion of mated females entering the fertilized female compartment depends on the effective mating of a wild male with a female, such proportion can be described by the probability $\frac{M}{M+M_s}$ for male-only releases, and $\frac{M}{M+M_s} \frac{F}{F+F_s}$ for both male and female releases. Our goal is to thoroughly analyze the related models using analytical methods whenever feasible, considering their complexity. If the manual analysis becomes intricate, we'll also use numerical simulations to enhance our understanding of these models.

3.1 Modeling of SIT with only sterile males releases

We start this progression with the 3-compartment model 3.1 while integrating the injection of sterile males into system 2.1. This 3-compartment model will provide valuable insights for further developments.

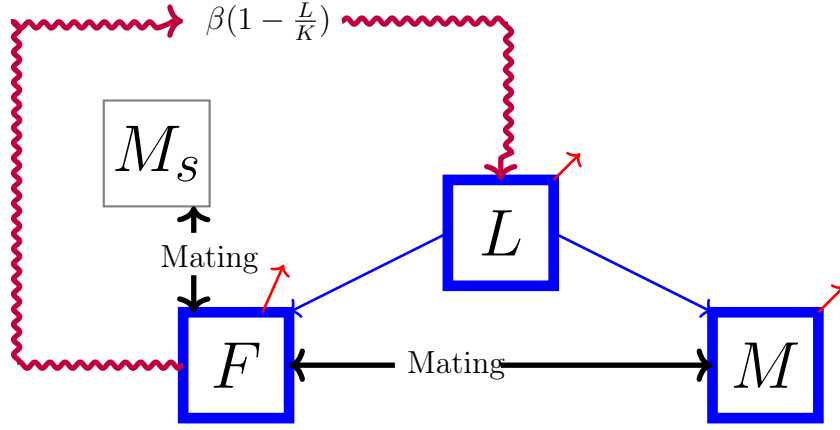


Figure 3.1: Diagram of the population model of *Drosophila sukukii*, corresponding to the system of equations 3.1 with sterile males releases

3.1.1 Inserting sterile males in the basic model

$$\begin{cases} \dot{L} = \beta \left(1 - \frac{L}{K}\right) v_F \left(\frac{M}{M+M_s}\right) F - (\mu_L + v_L) L \\ \dot{M} = v_L m L - \mu_M M \\ \dot{F} = v_L (1 - m) L - \mu_F F \end{cases} \quad (3.1)$$

I took M_s as a constant here, which can be described as a constant continuous release, but in reality, M_s population has its own dynamics and it can be changed depending on the number of sterile males released $\phi_1(t)$ in each time t , and the dynamics is $\dot{M}_s = \phi_1(t) - \mu_{M_s} M_s$

The subsequent models follow a similar analysis as the previous ones. Given that we have previously demonstrated the existence and uniqueness of the solution due to the Lipschitz nature of function f . Instead, our focus will shift directly to identifying equilibrium points and demonstrating their stability. Finally, we will complement our study by conducting simulations and drawing relevant conclusions.

Equilibrium points

$$\begin{cases} \dot{L} = 0 \\ \dot{M} = 0 \\ \dot{F} = 0 \end{cases} \implies \begin{cases} \beta \left(1 - \frac{L}{K}\right) v_F \left(\frac{M}{M+M_s}\right) F - (\mu_L + v_L) L = 0 \\ v_L m L - \mu_M M = 0 \\ v_L (1 - m) L - \mu_F F = 0 \end{cases}$$

After some basic calculations, we obtained the second-degree parabola:

$$\left[\eta_{05} \left(1 - \frac{L^*}{K}\right) - 1\right] L^* = \frac{M_s \mu_M}{v_L m} \quad (3.2)$$

with η_{05} as the basic reproduction number, and it is written as

$$\eta_{05} = \frac{(1 - m) v_L v_F \beta}{\mu_F (\mu_L + v_L)}$$

$$F^* = \frac{(1-m)v_L}{\mu_F} L^*$$

$$M^* = \frac{mv_L}{\mu_M} L^*$$

and with that, we see that if

- $M_s = 0$ we have two equilibrium points $E^* = (0, 0, 0)$ and $EE_1^* = (L_1^*, M_1^*, F_1^*)$ with $L_1^* = K(1 - \frac{1}{\eta_{05}})$ and thus if $\eta_{05} \leq 1$ we only have one equilibrium points which is E^* , else if $\eta_{05} > 1$ we have two equilibrium points E^* , and EE^* which is LAS, it is the same study as in the model 2.4.
- $M_s > 0$ the equilibrium points depends on the intersection of the curve $\zeta(L) = \alpha[\eta_{05}(1 - \frac{L^*}{K}) - 1]L^*$ and M_s while $\alpha = \frac{v_L m}{\mu_M}$ in this case we have two equilibrium points $EE_1^* = (L_1^*, M_1^*, F_1^*)$ and $EE_2^* = (L_2^*, M_2^*, F_2^*)$ in addition to the trivial equilibrium point $E^* = (0, 0, 0)$
- $M_s > \max(\zeta(L))$ in that case the trivial equilibrium point $E^* = (0, 0, 0)$ is the only equilibrium point we got

The two figures 3.2, and 3.3 describe the intersection between the number of sterile males released and its corresponding number of Larvas population at the equilibrium. We can see that starting from $M_s = 0$ until a certain number of releases $M_s < \max(\zeta(L))$ we have two equilibrium points. For a certain number of M_s released, we start getting imaginary roots, and thus we don't have real intersections.

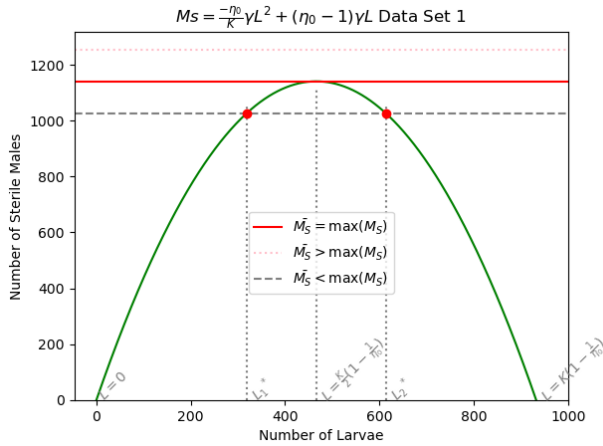


Figure 3.2: Intersection between The number of sterile Males released and the number of Larvas at the equilibrium (First set of Data)

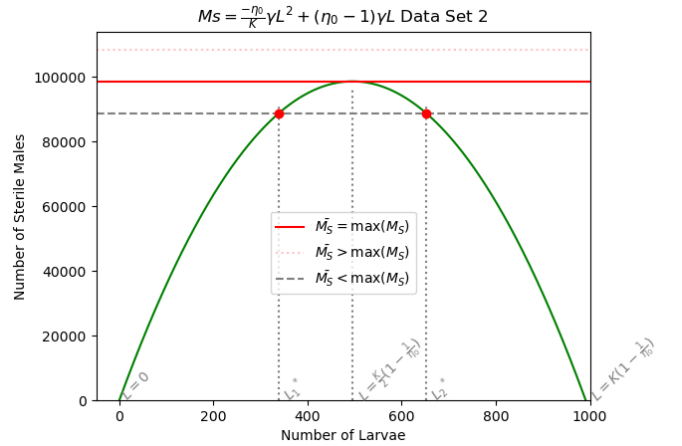


Figure 3.3: Intersection between The number of sterile Males released and the number of Larvas at the equilibrium (second set of Data)

Stability of the equilibrium

The Jacobian associated with the system is:

$$J = \begin{pmatrix} -\frac{\beta}{K} v_F \left(\frac{M}{M+M_s} \right) F - (\mu_L + v_L) & \beta \left(1 - \frac{L}{K} \right) v_F \left(\frac{M_s}{(M+M_s)^2} \right) F & \beta \left(1 - \frac{L}{K} \right) v_F \left(\frac{M}{M+M_s} \right) \\ v_L m & -\mu_M & 0 \\ v_L (1-m) & 0 & -\mu_F \end{pmatrix}$$

- for $E^* = (0, 0, 0)$

$$J(E^*) = \begin{pmatrix} -(\mu_L + v_L) & 0 & 0 \\ v_L m & -\mu_M & 0 \\ v_L(1-m) & 0 & -\mu_F \end{pmatrix}$$

which is always **asymptotically stable (AS)** and that comes from the fact that releasing sterile males will always affect the model and makes the $E^* = (0, 0, 0)$ AS regardless of the reproduction number.

- for $EE_1^* = (L_1^*, M_1^*, F_1^*) \neq 0$ and $EE_2^* = (L_2^*, M_2^*, F_2^*) \neq 0$

$$J = \begin{pmatrix} -\frac{\beta}{K} v_F \left(\frac{mv_L L}{mv_L L + \mu_M M_s} \right) \frac{(1-m)v_L L}{\mu_F} - (\mu_L + v_L) & \beta \left(1 - \frac{L}{K} \right) v_F \left(\frac{M_s}{(\frac{mv_L L}{\mu_M} + M_s)^2} \right) \frac{(1-m)v_L L}{\mu_F} & \beta \left(1 - \frac{L}{K} \right) v_F \left(\frac{M}{M+M_s} \right) \\ v_L m & -\mu_M & 0 \\ v_L(1-m) & 0 & -\mu_F \end{pmatrix}$$

changing M with M^* , F with F^* and putting $M_s = \alpha[\eta_{05}(1 - \frac{L^*}{K}) - 1]L^*$ and while $\alpha = \frac{v_L m}{\mu_M}$ we obtain

$$J = \begin{pmatrix} -\frac{(\mu_L + v_L)}{K} \left(\frac{L}{1 - \frac{L}{K}} \right) - (\mu_L + v_L) & \frac{\eta_{05}(1 - \frac{L}{K}) - 1}{\alpha \eta_{05}(1 - \frac{L}{K})} (\mu_L + v_L) & \beta \left(1 - \frac{L}{K} \right) v_F \left(\frac{M}{M+M_s} \right) \\ v_L m & -\mu_M & 0 \\ v_L(1-m) & 0 & -\mu_F \end{pmatrix}$$

To conclude the stability we will follow the **Proposition 2.2.1**. First, we will try to add a dimension to our system, such a dimension should help us only in the calculation and has no effect on the system. the additional dimension will make or Jacobian matrix a squared matrix.

The Jacobian in that case becomes:

$$J = \left(\begin{array}{ccc|cc} -\frac{(\mu_L + v_L)}{K} \left(\frac{L}{1 - \frac{L}{K}} \right) - (\mu_L + v_L) & \frac{\eta_{05}(1 - \frac{L}{K}) - 1}{\alpha \eta_{05}(1 - \frac{L}{K})} (\mu_L + v_L) & \beta \left(1 - \frac{L}{K} \right) v_F \left(\frac{M}{M+M_s} \right) & 0 & \\ v_L m & -\mu_M & 0 & 0 & \\ v_L(1-m) & 0 & -\mu_F & 0 & \\ 0 & 0 & 0 & 0 & -X \end{array} \right)$$

The matrix J is Metzler iff $\eta_{05} \left(1 - \frac{L}{K} \right) - 1 > 0$ and since it is a second-degree polynomial with a second derivative that is negative, we can conclude that the solutions of the second degree polynomial 3.5 are in the interval $0 < L^* < K \left(1 - \frac{1}{\eta_{05}} \right)$. Consequently, J is Metzler.

$$\text{We take } A = \begin{pmatrix} -\frac{(\mu_L + v_L)}{K} \left(\frac{L}{1 - \frac{L}{K}} \right) - (\mu_L + v_L) & \frac{\eta_{05}(1 - \frac{L}{K}) - 1}{\alpha \eta_{05}(1 - \frac{L}{K})} (\mu_L + v_L) \\ v_L m & -\mu_M \end{pmatrix}, \quad B = \begin{pmatrix} \beta \left(1 - \frac{L}{K} \right) v_F \left(\frac{M}{M+M_s} \right) & 0 \\ 0 & 0 \end{pmatrix},$$

$$C = \begin{pmatrix} v_L(1-m) & 0 \\ 0 & 0 \end{pmatrix}, \text{ and } D = \begin{pmatrix} -\mu_F & 0 \\ 0 & -X \end{pmatrix}$$

A is Metzler stable, the trace is negative it is Metzler because of the same reason why J is Metzler and a small verification will prove that $\det(A) > 0$.

we have to show that $D - CA^{-1}B$ is also Metzler and stable to conclude that we have stability, to do that we suppose first that $A^{-1} = \begin{pmatrix} a & b \\ c & d \end{pmatrix}$, and thus $D - CA^{-1}B =$

$$\begin{pmatrix} -\mu_F - av_L(1-m)\beta v_F(\frac{M}{M+M_s}) & 0 \\ 0 & -X \end{pmatrix}$$

we need to ensure that the $D - CA^{-1}B$ is Metzler stable, in this case, we have $a = \frac{-\mu_M}{\det(A)}$, and $D - CA^{-1}B$ is Metzler stable if the trace is negative and it's determinant is positive, while $\det(D - CA^{-1}B) = X\mu_F + Xav_L(1-m)\beta v_F(\frac{M}{M+M_s})$

First, since the $\det(A) > 0$, the trace is negative, and to conclude stability we have to show that $\det(D - CA^{-1}B) > 0$:

$$\begin{aligned} \left\{ \det(D - CA^{-1}B) > 0 \right\} &\implies \frac{\mu_M}{\det(A)} v_L(1-m)\beta v_F(\frac{M}{M+M_s}) < \mu_F \implies \left\{ \frac{L}{K}\eta_{05} > \eta_{05}(1 - \frac{L}{K}) - 1 \right. \\ &\implies \left\{ \eta_{05}(\frac{2L}{K} - 1) + 1 > 0 \right. \\ &\implies \left\{ \zeta'(L) = \eta_{05}(-\frac{2L}{K} + 1) - 1 < 0 \right. \end{aligned}$$

The stability at positive equilibrium points is determined by the sign of $\zeta'(L^*)$, which represents the slope of the parabola $\zeta(L) = [\eta_{05}(1 - \frac{L}{K}) - 1]L^*$ evaluated at these equilibria.

Thus,

- If $\zeta'(L^*) < 0$, meaning the equilibrium point is such that $L^* < \frac{K}{2} \left(1 - \frac{1}{\eta_{05}}\right)$, then the equilibrium is asymptotically stable.
- If $\zeta'(L^*) > 0$, meaning the positive equilibrium point is such that $L^* > \frac{K}{2} \left(1 - \frac{1}{\eta_{05}}\right)$, then the equilibrium is unstable.

Conclusion

This conclusion sums up all that we have talked about in this section and it is also supported by the bifurcation figures 3.9 and 3.10, and also the two figures above 3.2, and 3.3

- If $\eta_{05} \leq 1$, no existing positive solution, imaginary solution, the trivial equilibrium E^* is the unique equilibrium point of system 3.1, and E^* is locally asymptotically stable.
- If $\eta_{05} > 1$ and $M_S < \max(\zeta(L))$, 3.1 admits the trivial equilibrium E^* , which is locally asymptotically stable (LAS), as well as two endemic equilibria:

- (a) The endemic equilibrium EE_1^* such that $L^* < \frac{K}{2} \left(1 - \frac{1}{\eta_{05}}\right)$ is unstable.

(b) The endemic equilibrium EE_2^* such that $L^* > \frac{K}{2} \left(1 - \frac{1}{\eta_{05}}\right)$ is LAS.

- When $M_S > \max(\zeta(L))$, the trivial equilibrium E^* , which is locally asymptotically stable (LAS), is the only equilibrium of the system, and there is good reason to assume it is globally stable (GAS) for an abundant number of sterile males since the system always converges to extinction.
- In cases where $0 < M_S < \max(\zeta(L))$, both E^* and EE_2^* are stable, the demonstrated bistability implies that introductions of sterile males, even below the global eradication threshold, would control small invasions (but not large ones).

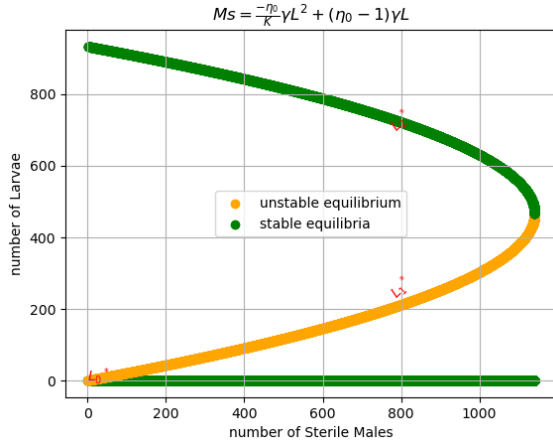


Figure 3.4: Bifurcation diagram of the stability points for the equilibrium points with SIT as a function of the number of sterile males M_s first data

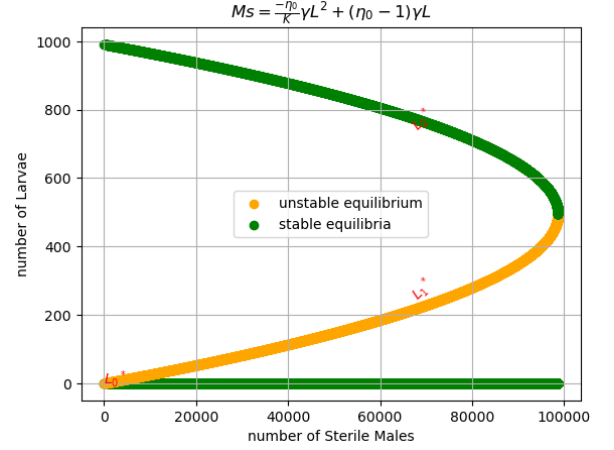


Figure 3.5: Bifurcation diagram of the stability points for the equilibrium points with SIT as a function of the number of sterile males M_s second data

Simulation

Figures 3.6 and 3.7 provide insight into population dynamics during the release of $M_s = 1200$ and $M_s = 100000$ respectively. These choices are guided by the bifurcation analyses illustrated in figures 3.9 and 3.10. Under the scenario of $M_s = 1200$, the first dataset reveals the presence of the trivial equilibrium point. Nevertheless, if we used the second dataset, the impact of such a release count on the population is minimal as it falls below the maximum point on the graph $\Gamma(L)$. This leads to the existence of two equilibrium points, and the dynamics ultimately converge to the second positive equilibrium point.

The simulation aligns harmoniously with the earlier analyzed analytical results, and eradicating the population in both datasets demands an extensive series of releases that could reach $M_s = 100,000$ sterile males, while we are starting with a small initial population of merely $L = 1000$, as depicted in figure 3.7.

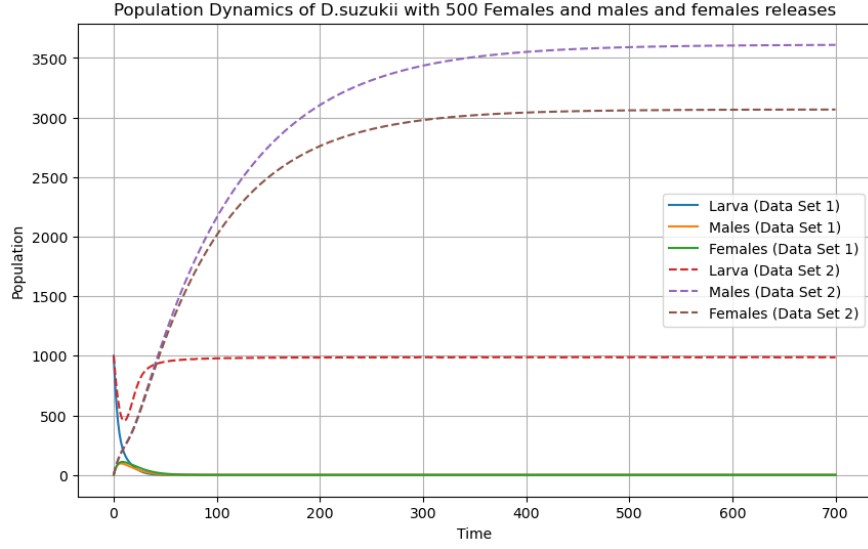


Figure 3.6: Simulation of the population evolution of *Drosophila suzukii*, in the TIS model 3.1, with continuous releases of sterile males ($M_S = 1200$) with an initial condition $L = 1000$, $M = 0$, and $F = 0$

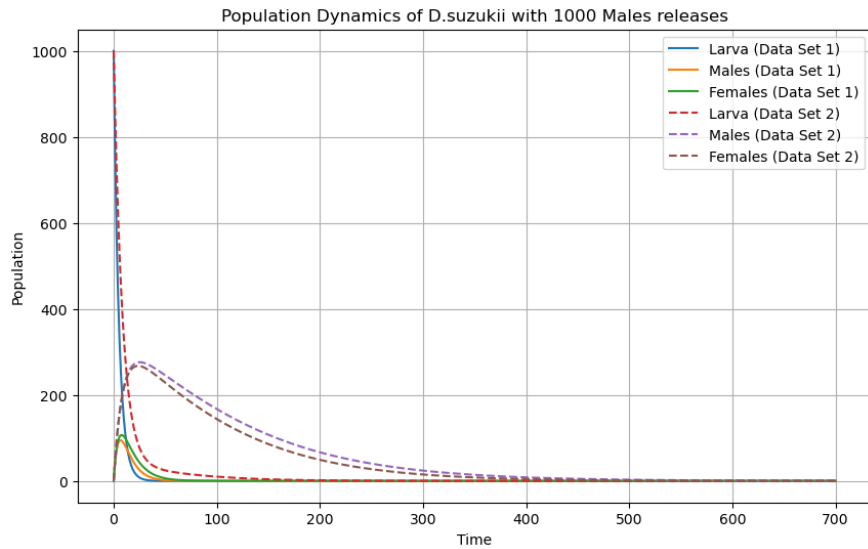


Figure 3.7: Simulation of the population evolution of *Drosophila suzukii*, in the TIS model 3.1, with continuous releases of sterile males ($M_S = 10000$) with an initial condition $L = 1000$, $M = 0$, and $F = 0$

3.1.2 6 compartments simplified model

In this sub-section, we will model the releasing of sterile males in the 6-compartment system 3.11 which will provide a clearer understanding of how different components interplay in the dynamics of *Drosophila suzukii*'s population, yet we will disregard the effect of female's re-mating ability that we will see in the forthcoming system 3.5. The prior model 3.1 treated sterile male dynamics as constant, neglecting their evolving behavior. However, these males possess their own dynamics, which we've integrated into the sixth dimension of the updated Equation 3.3. Our previous 3 compartment model also omitted some details, assuming females could reproduce by mating with wild males, disregarding the dynamics of females mated with sterile males or those not mated at all. To address this, we'll categorize females into three groups: "virgins" (V), females mated with sterile males (S), and females mated with wild males (F). The latter group significantly contributes to viable egg production for the next generation. These details serve to deepen our understanding of *Drosophila suzukii*'s dynamics, particularly in investigating female re-mating abilities (3.5).

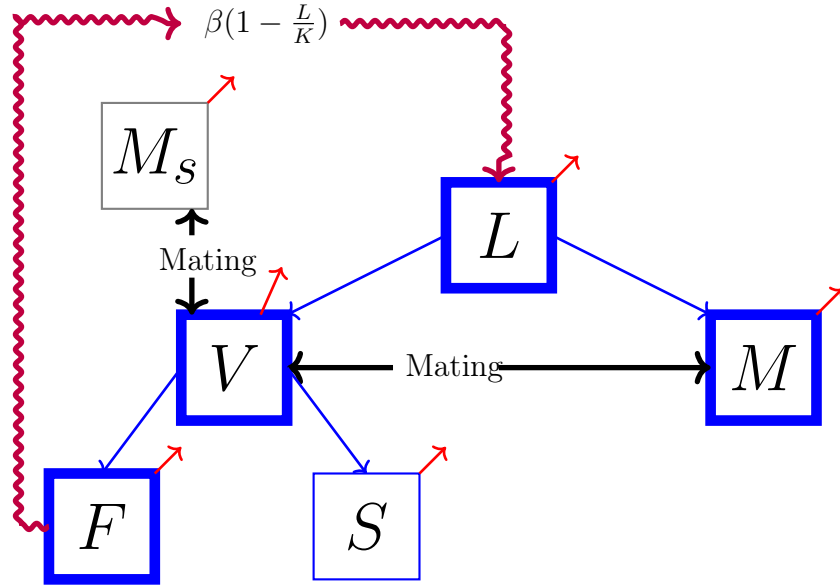


Figure 3.8: Diagram of the population model for TIS *Drosophila suzukii*, corresponding to the system of equations 3.3

Here we suppose that female mates once

$$\left\{ \begin{array}{l} \dot{L} = \beta \left(1 - \frac{L}{K} \right) F - (\mu_L + v_L) L \\ \dot{M} = v_L m L - \mu_M M \\ \dot{V} = v_L (1 - m) L - (\mu_F + v_F) V \\ \dot{S} = v_F \frac{M_s}{M + M_s} V - \mu_F S \\ \dot{F} = v_F \frac{M}{M + M_s} V - \mu_F F \\ \dot{M}_s = \phi_1(t) - \mu_{M_s} M_s \end{array} \right. \quad (3.3)$$

To streamline our analysis, we will assume that the dynamics of sterile males M_s remain constant, we can better explore the factors influencing female behavior and reproduction

without the added complexity of varying sterile male dynamics.

Equilibrium points

As the same case previously studied 3.1, the same method of calculations yields the equation:

$$[\eta_{06}(1 - \frac{L^*}{K}) - 1]L^* = \frac{M_s \mu_M}{v_L m} \quad (3.4)$$

$$3.4 \iff [\eta_{06}(1 - \frac{L^*}{K}) - 1] = \frac{M_s}{M^*}$$

with η_{06} as the basic reproduction number, and it is written as

$$\eta_{06} = \frac{(1 - m)v_L v_F \beta}{\mu_F (\mu_F + v_F) (\mu_L + v_L)}$$

$$F^* = \frac{\mu_L + v_L}{\beta(1 - \frac{L^*}{K})} L^*$$

$$M^* = \frac{m v_L}{\mu_M} L^*$$

$$V^* = \frac{\mu_F (M + M_s)}{v_F M} F^*$$

$$S^* = \frac{v_F}{\mu_F} \frac{M_s}{M_s + M} V = \frac{M_s}{M} F^*$$

we then have:

- if $M_s = 0$ then we fell in the previous system 2.4 where $S = 0$ with two equilibrium points each one defined by L^* while $L_0^* = 0$ and $L_1^* = K(1 - \frac{1}{\eta_{06}})$ as it has been previously mentioned
- if $M_s \neq 0$ the system has three equilibrium points the trivial equilibrium point $E^* = (0, 0, 0, 0, 0)$, $E_2^* = (L_1^*, V_1^*, S_1^*, F_1^*, M_1^*)$ and $E_1^* = (L_2^*, V_2^*, S_2^*, F_2^*, M_2^*)$ while L_1^* and L_2^* are solutions of 3.4, we can notice that the parabola 3.4 is the same as parabola 3.5 the difference between them lies in the reproduction number associated to each polynomial

Stability of the equilibrium

The Jacobian associated with the system 3.3

$$J = \begin{pmatrix} -(\mu_L + v_L) - \frac{\beta F^*}{K} & 0 & 0 & 0 & \beta(1 - \frac{L^*}{K}) \\ v_L m & -\mu_M & 0 & 0 & 0 \\ v_L(1 - m) & 0 & -(\mu_F + v_F) & 0 & 0 \\ 0 & -v_F \frac{M_s}{(M^* + M_s)^2} V^* & v_F \frac{M_s}{M^* + M_s} & -\mu_F & 0 \\ 0 & v_F \frac{M_s}{(M^* + M_s)^2} V^* & v_F \frac{M^*}{M^* + M_s} & 0 & -\mu_F \end{pmatrix}$$

NB : We can notice that S doesn't have an impact in other compartments and thus we can eliminate it from our matrix

$$J = \begin{pmatrix} -(\mu_L + v_L) - \frac{\beta F^*}{K} & 0 & 0 & \beta \left(1 - \frac{L^*}{K}\right) \\ v_L m & -\mu_M & 0 & 0 \\ v_L(1 - m) & 0 & -(\mu_F + v_F) & 0 \\ 0 & v_F \frac{M_s}{(M + M_s)^2} V & v_F \frac{M}{M + M_s} & -\mu_F \end{pmatrix}$$

- for $\eta_{06} \leq 1$ we have $E^* = (0, 0, 0, 0)$ as the only equilibrium point and thus, the Jacobian matrix becomes

$$J = \begin{pmatrix} -(\mu_L + v_L) & 0 & 0 & \beta \\ v_L m & -\mu_M & 0 & 0 \\ v_L(1 - m) & 0 & -(\mu_F + v_F) & 0 \\ 0 & 0 & 0 & -\mu_F \end{pmatrix}$$

we can notice that the fourth line contains many zeros, therefore, we can eliminate the fourth dimension since it can be related to a strictly negative eigenvalue, and thus taking into account the first three-by-three matrix, we can deduce that all its eigenvalues are negative. Thus, E^* is LAS, according to the **Hartman-Grobman theorem 2.1.1**.

- For E_2^* and E_1^* we will study the stability, using the **Metzler stability (Proposition:2.2.1)**.

following **proposition**, the matrix J can be divided to:

$$J = \left(\begin{array}{cc|cc} -(\mu_L + v_L) - \frac{\beta F^*}{K} & 0 & 0 & \beta \left(1 - \frac{L^*}{K}\right) \\ v_L m & -\mu_M & 0 & 0 \\ \hline v_L(1 - m) & 0 & -(\mu_F + v_F) & 0 \\ 0 & v_F \frac{M_s}{(M + M_s)^2} V & v_F \frac{M}{M + M_s} & -\mu_F \end{array} \right)$$

to deduce the stability. First, we have J as a Metzler Matrix let's take

$$A = \begin{pmatrix} -(\mu_L + v_L) - \frac{\beta F^*}{K} & 0 \\ v_L m & -\mu_M \end{pmatrix},$$

$$B = \begin{pmatrix} 0 & \beta \left(1 - \frac{L^*}{K}\right) \\ 0 & 0 \end{pmatrix},$$

$$C = \begin{pmatrix} v_L(1 - m) & 0 \\ 0 & v_F \frac{M_s}{(M + M_s)^2} V^* \end{pmatrix};$$

$$\text{and } D = \begin{pmatrix} -(\mu_F + v_F) & 0 \\ v_F \frac{M^*}{M + M_s} & -\mu_F \end{pmatrix}$$

applying **proposition 2.2.1** we can see that A is Metzler stable it is sufficient to prove that $D - CA^{-1}B$ is Metzler stable

we have

$$D - CA^{-1}B = \begin{pmatrix} -(\mu_F + v_F) & v_L(1 - m) \frac{\mu_M}{\det(A)} \beta \left(1 - \frac{L^*}{K}\right) \\ v_F \frac{M^*}{M + M_s} & -\mu_F + v_F \frac{M_s}{(M + M_s)^2} V^* \beta \left(1 - \frac{L^*}{K}\right) \frac{v_L m}{\det(A)} \end{pmatrix}$$

applying the fact that

$$F^* = \frac{\mu_L + v_L}{\beta(1 - \frac{L^*}{K})} L^*$$

and

$$V^* = \frac{\mu_F(M^* + M_s)}{v_F M^*} F^*$$

we obtain

$$\Rightarrow D - CA^{-1}B = \begin{pmatrix} -(\mu_F + v_F) & v_L(1 - m)\frac{\mu_M}{\det(A)}\beta(1 - \frac{L^*}{K}) \\ v_F\frac{M^*}{M^* + M_s} & -\mu_F + \mu_F\frac{M_s}{(M^* + M_s)}\mu_M(\mu_L + v_L)\frac{1}{\det(A)} \end{pmatrix}$$

and thus to show that this matrix is Metzler stable we must have $\text{trace}(D - CA^{-1}B) < 0$ and $\det(D - CA^{-1}B) > 0$ we will see the second condition first i.e.

$$\det(D - CA^{-1}B) = (\mu_F + v_F)\mu_F[1 - \frac{M_s}{(M^* + M_s)}\mu_M(\mu_L + v_L)\frac{1}{\det(A)}] - v_L(1 - m)\frac{\mu_M}{\det(A)}\beta(1 - \frac{L^*}{K})v_F\frac{M^*}{M^* + M_s} > 0$$

Alternatively we have:

$$3.4 \iff \eta_{06}(1 - \frac{L^*}{K})L^* = M_s\mu_m + v_LmL^*$$

then

$$\frac{M_s}{(M^* + M_s)} = \frac{\mu_M M_s}{(mv_L L^* + \mu_M M_s)} = \frac{M_s \mu_M}{\eta_{06}(1 - \frac{L^*}{K})L^*}$$

then:

$$\det(D - CA^{-1}B) = (\mu_F + v_F)\mu_F[\det(A) - \frac{M_s}{(M^* + M_s)}\mu_M(\mu_L + v_L)] - v_L(1 - m)\mu_M\beta(1 - \frac{L^*}{K})v_F\frac{M^*}{M^* + M_s} > 0$$

$$\iff \det(A) - \frac{M_s}{(M^* + M_s)}\mu_M(\mu_L + v_L) > \mu_M(\mu_L + v_L)\eta_{06}(1 - \frac{L^*}{K})\frac{M^*}{M^* + M_s}$$

while

$$\det(A) = \mu_M(\mu_L + v_L) + \mu_M\frac{\beta F^*}{K} = \mu_M(\mu_L + v_L) + \mu_M(\mu_L + v_L)\frac{L^*}{K}\frac{1}{(1 - \frac{L^*}{K})}$$

then

$$1 + \frac{L^*}{K}\frac{1}{(1 - \frac{L^*}{K})} - \frac{M_s}{M^* + M_s} > \eta_{06}(1 - \frac{L^*}{K})\frac{M^*}{M^* + M_s}$$

we obtain

$$\begin{aligned} \frac{L^*}{K}\frac{1}{(1 - \frac{L^*}{K})} &> \frac{M_s}{M^* + M_s} \\ \iff \frac{L^*}{K}\frac{1}{(1 - \frac{L^*}{K})} &> \frac{M_s\mu_M}{mv_L L^* \eta_{06}(1 - \frac{L^*}{K})} \\ \iff \frac{L^*}{K}mv_L L^* \eta_{06} &> M_s\mu_M \\ \iff -2\frac{\eta_{06}}{K}L^* + (\eta_{06} - 1) &< 0 \end{aligned}$$

CQFD which means we have $\det(D - CA^{-1}B) > 0$ iff $\Lambda'(L^*) < 0$ with $\Lambda(L^*) = [\eta_{06}(1 - \frac{L^*}{K}) - 1]L^*$ what is left showing that $\text{trace}(D - CA^{-1}B) < 0$

we have $\text{trace}(D - CA^{-1}B) = -(\mu_F + v_F) - \mu_F + \mu_F \frac{M_s}{(M^* + M_s)} \mu_M (\mu_L + v_L) \frac{1}{\det(A)} < 0$ which means $-(\mu_F + v_F) - u_F + \mu_F \frac{M_s}{(M^* + M_s)} \frac{1}{1 + \frac{L^*}{K} \frac{1}{(1 - \frac{L^*}{K})}}$ and because $\frac{1}{1 + \frac{L^*}{K} \frac{1}{(1 - \frac{L^*}{K})}} < 1$ and $\frac{M_s}{(M^* + M_s)}$ we have always $\text{trac}(D - CA^{-1}B) < 0$

Conclusion

- if $M_s = 0$ then we fell in the previous system 2.4 where $S = 0$ with two equilibrium points each one defined by L^* while $L_0^* = 0$ and $L_1^* = k(1 - \frac{1}{\eta_{06}})$ as it has previously mentioned and the analysis of the equilibrium points have already been studied see 3.1
- if $M_s \neq 0$ we have the same results as the previous model 3.1, it has either the trivial equilibrium point solely if we exceeded a certain releasing number $M_s < \max(\zeta(L))$ (see figures 3.2, 3.3, or three equilibrium points the trivial equilibrium point $E^* = (0, 0, 0, 0, 0)$, $E_2^* = (L_1^*, V_1^*, S_1^*, F_1^*, M_1^*)$ and $E_1^* = (L_2^*, V_2^*, S_2^*, F_2^*, M_2^*)$ while L_1^* and L_2^* are solutions of 3.4 and $M_s > \max(\zeta(L))$.
- $E^* = (0, 0, 0, 0, 0)$ is always LAS
- for $E_2^* = (L_1^*, V_1^*, S_1^*, F_1^*, M_1^*)$ and $E_1^* = (L_2^*, V_2^*, S_2^*, F_2^*, M_2^*)$ while L_1^* and L_2^* are solutions of 3.4, we use the intersection between the two curves to find the equilibrium points
 $\Gamma(M_s) = \frac{M_s \mu_M}{v_L m}$ and $\Lambda(L^*) = [\eta_{06}(1 - \frac{L^*}{K}) - 1]L^*$
 and the stability related with the point L^* in which $\Lambda'(L^*) < 0$ with $\Lambda(L^*) = [\eta_{06}(1 - \frac{L^*}{K}) - 1]L^*$

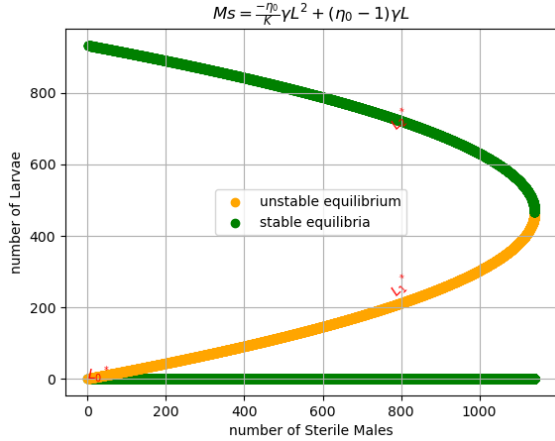


Figure 3.9: Bifurcation diagram of the stability points for the equilibrium points with SIT as a function of the number of sterile males M_s first data

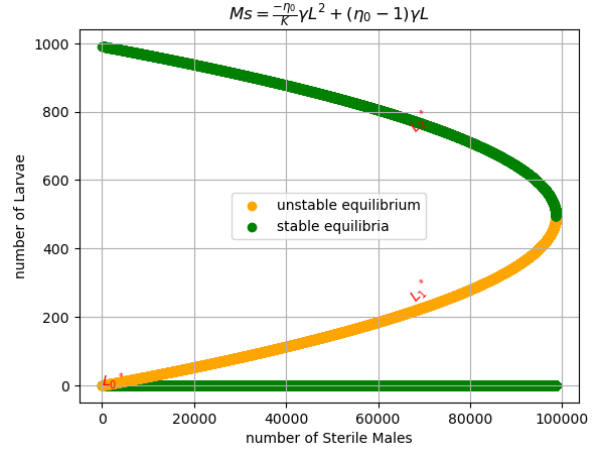


Figure 3.10: Bifurcation diagram of the stability points for the equilibrium points with SIT as a function of the number of sterile males M_s second data

The introduction of the new compartments S to the problem will not impact the equilibrium points. This is because S does not interact with any other compartment.

3.1.3 Model Incorporating the re-mating Ability in the 6 Compartments model

In this model, we change the hypothesis of single mating for females in the system 3.3, allowing females to re-mate. This ability is modeled with a proportion of the females that come back to the virgin compartment, such a proportion is modeled by δ and γ .

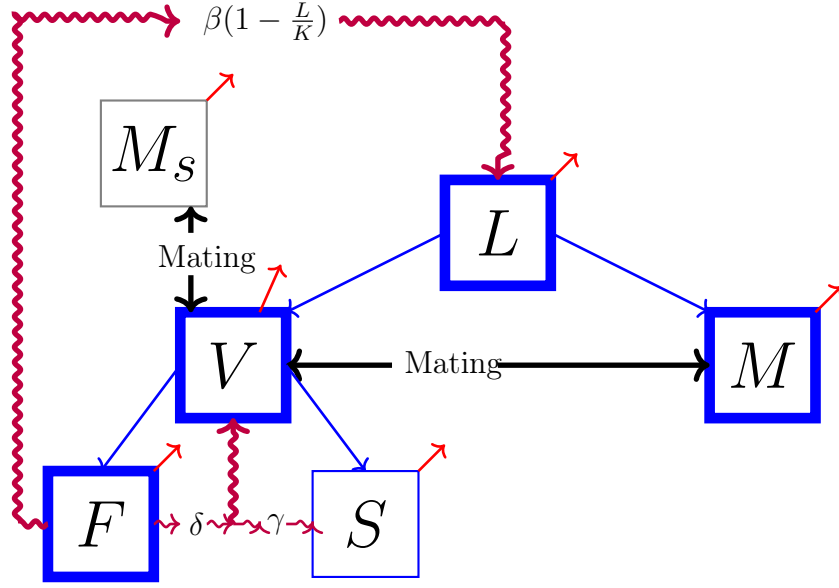


Figure 3.11: Diagram of the population model for TIS *Drosophila suzukii*, corresponding to the system of equations 3.5

We obtain the following model

$$\begin{cases} \dot{L} = \beta \left(1 - \frac{L}{K}\right) F - (\mu_L + v_L) L \\ \dot{M} = v_L m L - \mu_M M \\ \dot{V} = v_L (1 - m) L + \delta F + \gamma S - (\mu_F + v_F) V \\ \dot{S} = v_F \frac{M_s}{M + M_s} V - (\gamma + \mu_F) S \\ \dot{F} = v_F \frac{M}{M + M_s} V - (\mu_F + \delta) F \\ \dot{M}_s = \phi_1(t) - \mu_{M_s} M_s \end{cases} \quad (3.5)$$

Equilibrium points

Searching for the equilibrium point will lead us to the following degree two polynomial

$$\left[\eta_{07} \left(1 - \frac{L^*}{K}\right) + \frac{\delta v_F}{\mu_F (\mu_F + v_F)} - \frac{(\mu_F + \delta)}{\mu_F} \right] L^* = \left[\frac{(\mu_F + \delta)}{\mu_F} - \frac{\gamma v_F (\mu_F + \delta) \mu_F}{(\mu_F + \gamma) (\mu_F + v_F)} \right] \frac{M_s \mu_M}{m v_L} \quad (3.6)$$

with η_{07} as the basic reproduction number, and it is written as

$$\eta_{07} = \frac{(1 - m) v_L v_F \beta}{\mu_F (\mu_F + v_F) (\mu_L + v_L)}$$

$$F^* = \frac{\mu_L + v_L}{\beta \left(1 - \frac{L^*}{K}\right)} L^*$$

$$M^* = \frac{m v_L}{\mu_M} L^*$$

$$S^* = \frac{M_s (\mu_F + \delta)}{M (\mu_F + \gamma)} \frac{(\mu_L + v_L)}{\beta \left(1 - \frac{L^*}{K}\right)} L^* = \frac{M_s \mu_M (\mu_F + \delta)}{m v_L (\mu_F + \gamma)} \frac{(\mu_L + v_L)}{\beta \left(1 - \frac{L^*}{K}\right)}$$

$$V^* = \frac{(\mu_F + \delta)}{v_F} \left(1 + \frac{M_s \mu_M}{m v_L L^*}\right) \frac{\mu_L + v_L}{\beta \left(1 - \frac{L^*}{K}\right)} L^*$$

we then have:

- if $M_s = 0$ then we fell in the previous system 2.8 where $S = 0$ and $\gamma = 0$ with two equilibrium points $L_0^* = 0$ and L_1^* as it has previously mentioned
- if $M_s \neq 0$ the system has:
 - The trivial equilibrium point $E^* = (0, 0, 0, 0, 0)$ as the only equilibrium point, if the number of sterile males released has exceeded a certain number $M_s^* < M_s$ (see figures 3.12, and 3.13 the orange dotted line)
 - Three equilibrium points: the trivial equilibrium point $E^* = (0, 0, 0, 0, 0)$, $E_2^* = (L_1^*, V_1^*, S_1^*, F_1^*, M_1^*)$ and $E_1^* = (L_2^*, V_2^*, S_2^*, F_2^*, M_2^*)$ while L_1^* and L_2^* are solutions of 3.6, (the orange dotted line in the figures 3.12, and 3.13)

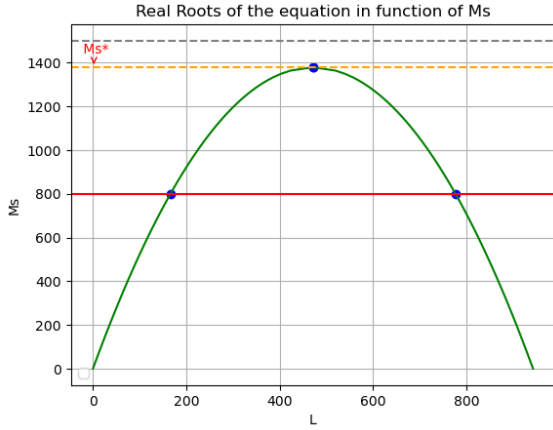


Figure 3.12: Intersection of Larva equilibrium points curve with one of the males release complex model

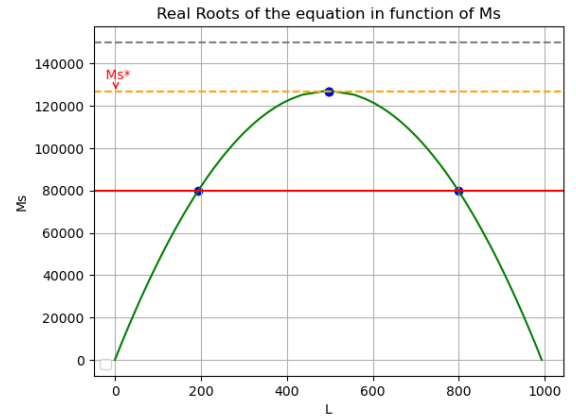


Figure 3.13: Intersection of Larva equilibrium points curve with one of the males release complex model

Stability studies of the Equilibrium points

The Jacobian matrix is defined by:

$$J = \begin{pmatrix} -(\mu_L + v_L) - \frac{\beta F^*}{K} & 0 & 0 & 0 & \beta \left(1 - \frac{L^*}{K}\right) \\ v_L m & -\mu_M & 0 & 0 & 0 \\ v_L (1 - m) & 0 & -(\mu_F + v_F) & \gamma & \delta \\ 0 & -v_F \frac{M_s}{(M + M_s)^2} V & v_F \frac{M_s}{M + M_s} & -(\mu_F + \gamma) & 0 \\ 0 & v_F \frac{M_s}{(M + M_s)^2} V & v_F \frac{M}{M + M_s} & 0 & -(\mu_F + \delta) \end{pmatrix}$$

We can notice that we cannot get rid of the S compartment this time because it interacts with the V compartment therefore J is not a Metzler matrix

- For $E^* = (0, 0, 0, 0, 0)$ we have that

$$J(E^*) = \begin{pmatrix} -(\mu_L + v_L) & 0 & 0 & 0 & \beta \\ v_L m & -\mu_M & 0 & 0 & 0 \\ v_L(1 - m) & 0 & -(\mu_F + v_F) & \gamma & \delta \\ 0 & 0 & v_F & -(\mu_F + \gamma) & 0 \\ 0 & 0 & 0 & 0 & -(\mu_F + \delta) \end{pmatrix}$$

The last row has many zeros so we can study only the 4×4 matrix, which is the matrix that contains the four first lines and columns. Using the proposition about the stability of the Metzler matrix we can see that $A = \begin{pmatrix} -(\mu_L + v_L) & 0 \\ v_L m & -\mu_M \end{pmatrix}$ is Metzler stable, and $B = 0_{M_4}$ thus the stability condition of the equilibrium point is based on the determinant of $D = \begin{pmatrix} -(\mu_F + v_F) & \gamma \\ v_F & -(\mu_F + \gamma) \end{pmatrix}$ and then E^* is stable $\iff (\mu_F + \gamma)(\mu_F + v_F) > \gamma v_F$ $\iff 1 > \frac{\gamma v_F}{(\mu_F + \gamma)(\mu_F + v_F)}$. As we will see in the numerical simulation for both datasets we have that E^* is always locally stable.

- For the other two equilibrium points we will proceed to the numerical stability study because it is hard to analyze it mathematically (see the simulation section).

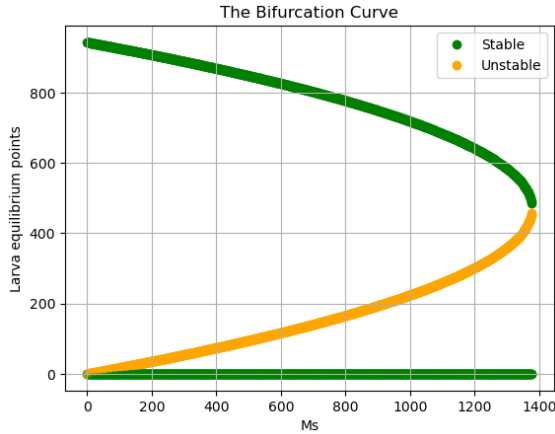


Figure 3.14: Bifurcation diagram of the stability points for the equilibrium points with SIT as a function of the number of sterile males M_s first data

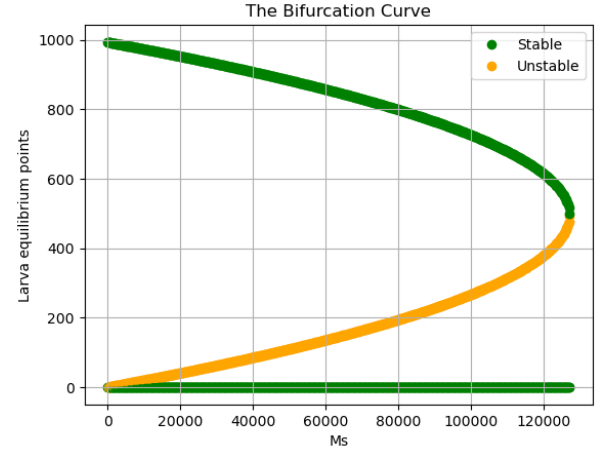


Figure 3.15: Bifurcation diagram of the stability points for the equilibrium points with SIT as a function of the number of sterile males M_s second data

Simulation

Before delving into the simulation analysis, it's imperative to establish the stability of the trivial equilibrium point, denoted as E^* . In the context of the first dataset, the inequality $\frac{\gamma v_F}{(\mu_F + \gamma)(\mu_F + v_F)} = 0.49 < 1$ holds, and for the second dataset, it stands at $\frac{\gamma v_F}{(\mu_F + \gamma)(\mu_F + v_F)} = 0.87 < 1$. As a result, we can confidently conclude that E^* remains locally stable.

The choice of utilizing $M_s = 80000$ in the simulation is strategically selected to achieve two objectives simultaneously. Supporting the analytical analysis, and ensuring the convergence

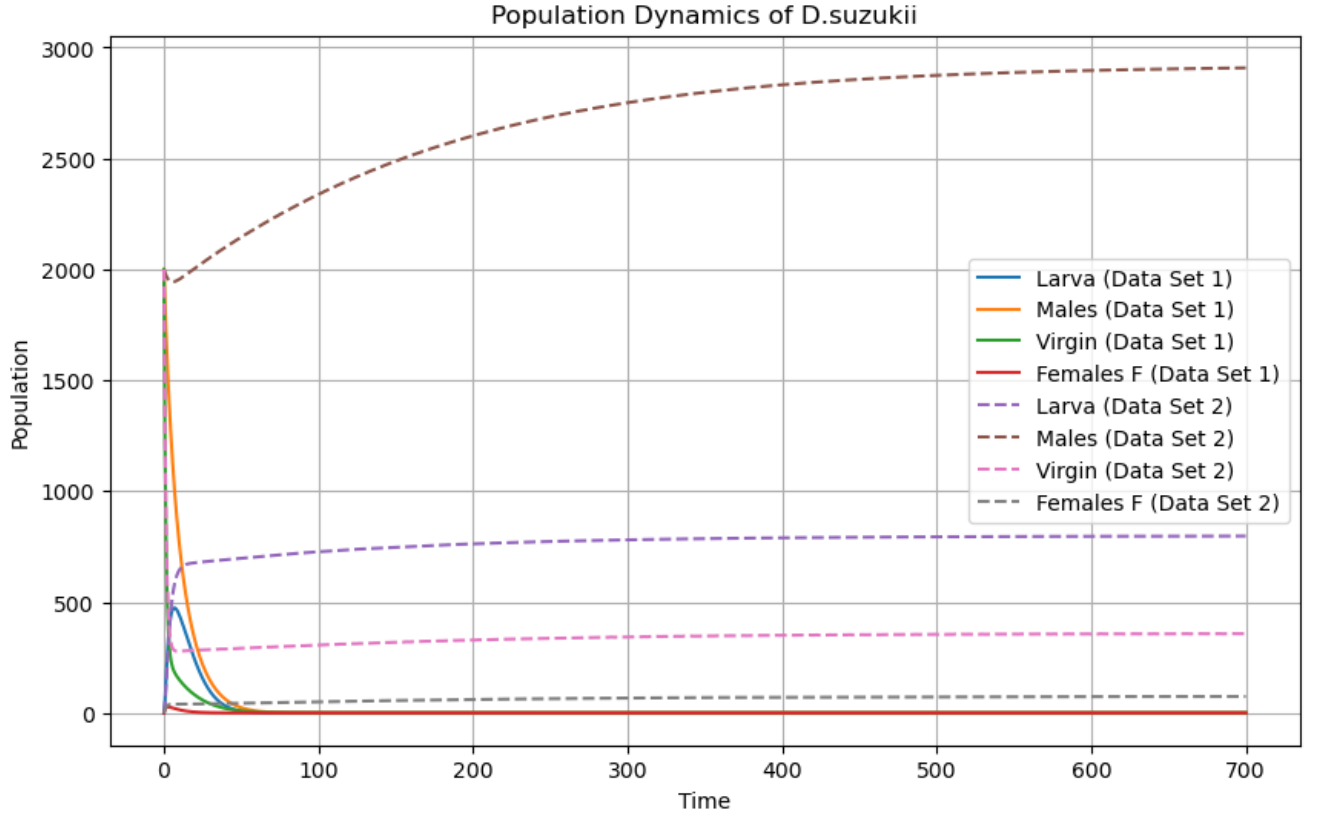


Figure 3.16: Population dynamics with Releasing $M_s = 80000$ Males continuously , $M = 2000$ $V = 2000$

of each dataset to a distinct equilibrium point. Supported by the evidence from bifurcation figures 3.14 and 3.15, when employing $M_s = 80000$, eradication is accomplished for the first dataset. Meanwhile, convergence to a positive population of $L^* = 800$ larvae is achieved for the second dataset. These outcomes are illustrated in the population dynamics depicted in figure 3.16.

The numerical stability analysis in the two bifurcation figures 3.14 and 3.15 supported the analytical analysis about having two equilibrium points for each number of releases of males in addition to the trivial equilibrium point. Additionally, they provide us with a stability analysis that we couldn't do analytically, one of the two equilibrium points that we have is stable (green) and the other one is unstable (yellow).

Throughout more examination of the recent bifurcation figures, namely 3.14 and 3.15, we are under the necessity for $M_s > 1400$ in the first dataset and $M_s \geq 130000$ in the second dataset to establish E^* as the unique equilibrium point. In contrast, the prior systems outlined in equations 3.1 and 3.3, as observed in bifurcation figures 3.9 and 3.10, demand a lesser number of releases to converge solely to the trivial equilibrium point. This phenomenon is due to the unique capability of female remating. The ability to remate translates to a higher offspring number, subsequently resulting in a larger wild population that requires suppression. This demand for suppression can be effectively addressed through an increased number of releases.

3.2 Releasing sterile Females and Males

Simultaneous release of males and females introduces complexity and poses challenges for modeling. We start with a 3-compartment model, analyzing equilibria, stability, and simulations. In the subsequent models, we introduce hypotheses incrementally, and we expand the calculations comprehensively.

3.2.1 Embracing sterile Females and Males releases in the Basic Model

The basic model always serves as our starting point. To account for the introduction of released males and females, we modify the mating probability in 2.1. This adjustment is quantified using the mathematical expression $\left(\frac{M}{M+M_s}\right)\left(\frac{F}{F+F_s}\right)$, which captures the combined probability of a mating male and a mated female belonging to their respective fertile groups. This joint likelihood is crucial for a successful mating event to contribute to future generations. Thus, we arrive at the resultant model through these considerations.

$$\begin{cases} \dot{L} = \beta \left(1 - \frac{L}{K}\right) v_F \left(\frac{M}{M+M_s}\right) \left(\frac{F}{F+F_s}\right) F - (\mu_L + v_L) L \\ \dot{M} = v_L m L - \mu_M M \\ \dot{F} = v_L (1 - m) L - \mu_F F \end{cases} \quad (3.7)$$

Equilibrium points

The equilibrium points of the system 3.7 depend on the solution of the third-degree polynomial described by:

$$m(1 - m)v_L^2[\eta_{08}(1 - \frac{L^*}{K}) - 1](L^*)^2 - [M_s\mu_M(1 - m)v_L + F_s\mu_F m v_L]L^* = M_s F_s \mu_M \mu_F \quad (3.8)$$

$$3.8 \iff (1) \quad -m(1-m)\frac{\eta_{08}}{K}v_L^2(L^*)^3 + m(1-m)v_L^2(\eta_{08}-1)(L^*)^2 - [M_s\mu_M(1-m)v_L + F_s\mu_F m v_L]L^* = M_s F_s \mu_M \mu_F$$

$$3.8 \iff (2) \quad FM[\eta_{08}(1 - \frac{L^*}{K}) - 1] - [M_s F + F_s M] = M_s F_s$$

$$3.8 \iff (3) \quad \eta_{08}(1 - \frac{L^*}{K}) = \frac{(F + F_s)(M + M_s)}{FM}$$

with η_{08} as the basic reproduction number, and it is written as

$$\eta_{08} = \frac{(1 - m)v_L v_F \beta}{\mu_F (\mu_L + v_L)}$$

$$F^* = \frac{(1 - m)v_L}{\mu_F} L^*$$

$$M^* = \frac{mv_L}{\mu_M} L^*$$

(1), (2), and (3) are different versions of 3.8 they are useful in the stability analysis.

In order to determine whether we have a negative equilibrium point or not, we will divide our polynomial into two equations

$$\zeta_1(L) = -\frac{\eta_{08}}{K}m(1-m)v_L^2L^3 + m(1-m)v_L^2(\eta_{08}-1)L^2 \quad (3.9)$$

and the affine equation

$$\Gamma(L) = [M_s\mu_M(1-m)v_L + F_s\mu_Fmv_L]L + M_sF_s\mu_F\mu_M \quad (3.10)$$

see figures: 3.17, and 3.18. The intersections of these two curves are our equilibrium points. First we can notice that the table of variation of 3.9 between $]-\infty, 0]$ for $(\eta_{08}-1) > 0$ is given by

x	$-\infty$	0
$\zeta'_1(x)$	$-$	
$\zeta_1(x)$	$+\infty$	0

we can notice also through 3.10 that $\Gamma(L)$ is increasing with L , and that if $L = 0$ we have that $M_sF_s\mu_F\mu_M > 0$ and thus we always have one negative intersection between Γ and ζ_1 , which gives a negative equilibrium point.

Conclusion:

- let $M_s = 0$ and $F_s = 0$ we obtain exactly our previous problem 2.1 related to the male abundance and $\gamma = 1$, in that case, we have two equilibrium points

$E^* = (0, 0, 0)$ and $EE_1^* = (L_1^*, M_1^*, F_1^*)$ with $L_1^* = k(1 - \frac{1}{\eta_{08}})$, and thus we already proved that, if $\eta_{08} \leq 1$ we only have one equilibrium points which is E^* else if $\eta_{08} > 1$ we have two equilibrium points and EE^* is LAS

- let $M_s \neq 0$ and $F_s = 0$ the equilibrium points, in addition to the trivial equilibrium point, depending on the intersection of the curve $\zeta(L) = \alpha[\eta_{08}(1 - \frac{L^*}{K}) - 1]L^*$ and M_s while $\alpha = \frac{v_L m}{\mu_M}$ (already discussed in 3.5)
- let $M_s \neq 0$ and $F_s \neq 0$: We consider $N = F_s + M_s$ the number of the released population, with $F_s = \frac{N}{2}$, and based on this number various intersections between ζ_1 and Γ arise, leading to the subsequent scenarios (see figures: 3.17, and 3.18):

- let $0 < N < N^*$ (blue curve): In addition to the trivial equilibrium point $E^* = (0, 0, 0)$, we have three equilibrium points, one of them is negative (to be neglected), and two others are positive ones. The number of Larva related to the equilibrium is the intersection of the curve

$$\zeta_1(L) = -\frac{\eta_{08}}{K}m(1-m)v_L^2L^3 + m(1-m)v_L^2(\eta_{08} - 1)L^2$$

and

$$\Gamma(L) = [M_s\mu_M(1-m)v_L + F_s\mu_Fmv_L]L + M_sF_s\mu_F\mu_M$$

- let $N^* < N$ (green curve), the trivial equilibrium point $E^* = (0, 0, 0)$ is the only equilibrium point we got.

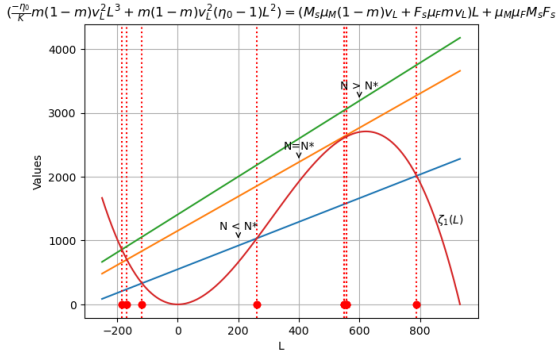


Figure 3.17: Intersections between the two graphs $\zeta_1(L)$ (in red) and Γ for different values of the released population $N = 500$ (blue), $N = 724$ (orange), and $N = 800$ green. The red dots represent the intersection points. (first data set)

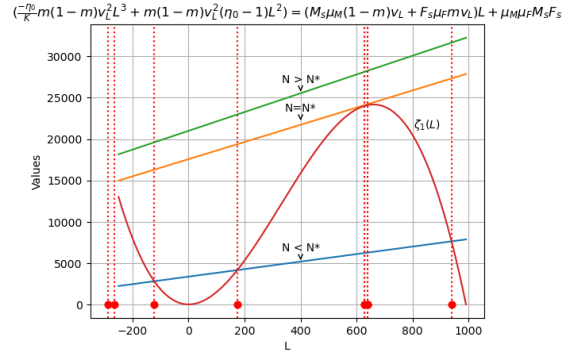


Figure 3.18: Intersections between the graphs of $\zeta(L)$ (in red) and Γ for different values of the released population $N = 10000$ (blue), $N = 22870$ (orange), and $N = 25000$ green. The red dots represent the intersection points. (second data set)

Stability analysis

The Jacobian associated with the system 3.7:

$$J = \begin{bmatrix} -\frac{\beta}{K}v_F \left(\frac{M}{M+M_s} \right) \left(\frac{F}{F+F_s} \right) F - (\mu_L + v_L) & \beta \left(1 - \frac{L}{K} \right) v_F \left(\frac{M_s}{(M+M_s)^2} \right) \left(\frac{F}{F+F_s} \right) F & \beta \left(1 - \frac{L}{K} \right) v_F \left(\frac{2FF_s+F^2}{(F+F_s)^2} \right) \left(\frac{M}{M+M_s} \right) \\ v_L m & -\mu_M & 0 \\ v_L(1-m) & 0 & -\mu_F \end{bmatrix}$$

- For the trivial equilibrium point $E^* = (0, 0, 0)$ we have that

$$J(E^*) = \begin{pmatrix} -(\mu_L + v_L) & 0 & 0 \\ v_L m & -\mu_M & 0 \\ v_L(1-m) & 0 & -\mu_F \end{pmatrix}$$

and obviously, all the eigenvalues are negative, and thus the trivial equilibrium point is always LAS

To study the stability of the positive equilibrium points we will transform the Jacobian into a 4 dimension matrix and then we will apply the Metzler proposition stated before.

we obtain

$$J = \begin{bmatrix} -\frac{\beta}{K}v_F \left(\frac{M}{M+M_s}\right) \left(\frac{F}{F+F_s}\right) F - (\mu_L + v_L) & \beta \left(1 - \frac{L}{K}\right) v_F \left(\frac{M_s}{(M+M_s)^2}\right) \left(\frac{F}{F+F_s}\right) F & \beta \left(1 - \frac{L}{K}\right) v_F \left(\frac{2FF_s+F^2}{(F+F_s)^2}\right) \left(\frac{M}{M+M_s}\right) & 0 \\ v_L m & -\mu_M & 0 & 0 \\ v_L(1-m) & 0 & -\mu_F & 0 \\ 0 & 0 & 0 & -X \end{bmatrix}$$

Next, we will prove that J is Metzler stable in the same way we previously concluded, J can be viewed as

$$J = \left[\begin{array}{ccc|cc} -\frac{\beta}{K}v_F \left(\frac{M}{M+M_s}\right) \left(\frac{F}{F+F_s}\right) F - (\mu_L + v_L) & \beta \left(1 - \frac{L}{K}\right) v_F \left(\frac{M_s}{(M+M_s)^2}\right) \left(\frac{F}{F+F_s}\right) F & \beta \left(1 - \frac{L}{K}\right) v_F \left(\frac{2FF_s+F^2}{(F+F_s)^2}\right) \left(\frac{M}{M+M_s}\right) & 0 & 0 \\ v_L m & -\mu_M & 0 & 0 & 0 \\ v_L(1-m) & 0 & -\mu_F & 0 & 0 \\ 0 & 0 & 0 & -X & 0 \end{array} \right]$$

and therefore by calculating the $D - CA^{-1}B$ we obtain a matrix that looks like

$$D - CA^{-1}B = \begin{pmatrix} -\mu_F + \frac{\mu_M}{\det(A)}v_L(1-m)\beta \left(1 - \frac{L}{K}\right) v_F \left(\frac{2FF_s+F^2}{(F+F_s)^2}\right) \left(\frac{M}{M+M_s}\right) & 0 \\ 0 & -X \end{pmatrix}$$

to conclude the stability we have to show that $\text{trace}(D - CA^{-1}B) < 0$ which equivalent to $-\mu_F + \frac{\mu_M}{\det(A)}v_L(1-m)\beta \left(1 - \frac{L}{K}\right) v_F \left(\frac{2FF_s+F^2}{(F+F_s)^2}\right) \left(\frac{M}{M+M_s}\right) < 0$

while

$$A = \begin{pmatrix} -\frac{\beta}{K}v_F \left(\frac{M}{M+M_s}\right) \left(\frac{F}{F+F_s}\right) F - (\mu_L + v_L) & \beta \left(1 - \frac{L}{K}\right) v_F \left(\frac{M_s}{(M+M_s)^2}\right) \left(\frac{F}{F+F_s}\right) F \\ v_L m & -\mu_M \end{pmatrix}$$

$$\iff A = \begin{pmatrix} -\frac{\beta}{K}v_F \left(\frac{1}{\eta_{08}(1-\frac{L}{K})}\right) F - (\mu_L + v_L) & \beta \left(1 - \frac{L}{K}\right) v_F \left(\frac{M_s}{(M+M_s)}\right) \left(\frac{F}{F+F_s}\right) \left(\frac{1}{M+M_s}\right) F \\ v_L m & -\mu_M \end{pmatrix}$$

and thus $\det(A) = (\mu_L + v_L)\mu_M[\eta_{08}\frac{L}{K}\left(\frac{1}{\eta_{08}(1-\frac{L}{K})}\right) + 1 - \eta_{08}(1 - \frac{L}{K})\left(\frac{1}{\eta_{08}(1-\frac{L}{K})}\right)\frac{M_s}{M+M_s}]$

$$\text{trace}(D - CA^{-1}B) < 0 \iff -\mu_F + \frac{\mu_M}{\det(A)}v_L(1-m)\beta \left(1 - \frac{L}{K}\right) v_F \left(\frac{2FF_s+F^2}{(F+F_s)^2}\right) \left(\frac{M}{M+M_s}\right) < 0$$

$$\iff -\mu_F + \mu_F(\mu_L + v_L)\frac{\mu_M}{\det(A)}\eta_{08}\left(1 - \frac{L}{K}\right) \left(\frac{2F_s+F}{(F+F_s)}\right) \left(\frac{F}{(F+F_s)}\right) \left(\frac{M}{M+M_s}\right) < 0$$

$$\iff (\mu_L + v_L)\mu_M\eta_{08}\left(1 - \frac{L}{K}\right) \left(\frac{2F_s+F}{(F+F_s)}\right) \left(\frac{F}{(F+F_s)}\right) \left(\frac{M}{M+M_s}\right) < \det(A)$$

taking into account (3) we obtain

$$\begin{aligned} \iff (\mu_L + v_L)\mu_M\eta_{08} \left(1 - \frac{L}{K}\right) \left(\frac{2F_s + F}{(F + F_s)}\right) \left(\frac{1}{\eta_{08} \left(1 - \frac{L}{K}\right)}\right) < \det(A) \\ \iff (\mu_L + v_L)\mu_M \left(\frac{2F_s + F}{(F + F_s)}\right) < \det(A) \end{aligned}$$

using $\det(A)$ expression we get

$$\begin{aligned} (\mu_L + v_L)\mu_M \left(\frac{2F_s + F}{(F + F_s)}\right) < (\mu_L + v_L)\mu_M \left[\eta_{08} \frac{L}{K} \left(\frac{1}{\eta_{08} \left(1 - \frac{L}{K}\right)}\right) + 1 - \eta_{08} \left(1 - \frac{L}{K}\right) \left(\frac{1}{\eta_{08} \left(1 - \frac{L}{K}\right)}\right) \frac{M_s}{M + M_s}\right] \\ \iff \frac{2F_s + F}{(F + F_s)} < \eta_{08} \frac{L}{K} \left(\frac{1}{\eta_{08} \left(1 - \frac{L}{K}\right)}\right) + 1 - \frac{M_s}{M + M_s} \end{aligned}$$

after small changes, we obtain

$$\begin{aligned} \left(1 + \frac{F_s}{F_s + F}\right) + \frac{M_s}{M + M_s} < \frac{L}{K} \frac{1}{\left(1 - \frac{L}{K}\right)} + 1 \iff \left(\frac{F_s}{F_s + F} + \frac{M_s}{M + M_s}\right) < \frac{L}{K} \frac{1}{\left(1 - \frac{L}{K}\right)} \\ \iff \frac{F_s(M + M_s) + (F_s + F)M_s}{(F_s + F)(M + M_s)} < \frac{L}{K} \frac{1}{\left(1 - \frac{L}{K}\right)} \end{aligned}$$

using (2) we obtain:

$$\begin{aligned} 2M_s F_s + M_s F + M F_s < F M \eta_{08} \frac{L}{K} \\ \iff 2FM[(\eta_{08} - 1) - \frac{L}{K}\eta_{08}] - M_s F - M F_s < FM\eta_{08} \frac{L}{K} \\ \iff 2FM(\eta_{08} - 1) - 3FM \frac{L}{K} \eta_{08} - M_s F - M F_s < 0 \end{aligned}$$

Now we use the values of the equilibrium points we obtain

$$\iff -3m(1 - m)v_L^2 \frac{\eta_{08}}{K} L^3 + 2(\eta_{08} - 1)m(1 - m)v_L^2 L^2 - [M_s \mu_M(1 - m)v_L + F_s \mu_F m v_L]L < 0$$

$$\iff -3m(1 - m)v_L^2 \frac{\eta_{08}}{K} L^2 + 2(\eta_{08} - 1)m(1 - m)v_L^2 L - [M_s \mu_M(1 - m)v_L + F_s \mu_F m v_L] < 0$$

To fulfill the stability we must have $\zeta'(L) < 0$ with $\zeta(L) = m(1 - m)v_L^2 \frac{\eta_{08}}{K} L^3 + (\eta_{08} - 1)m(1 - m)v_L^2 L^2 - [M_s \mu_M(1 - m)v_L + F_s \mu_F m v_L]L$ defined by 3.8

then the stable equilibrium point is the one in which the derivative of the third-degree polynomial 3.8 is negative.

Conclusion

Depending on the values of the released population we obtain different intersections between ζ_1 and Γ , we fall into the following cases (see figures 3.19, and 3.20):

- Let $N < N^*$: In addition to the trivial equilibrium point, the intersection gives three other equilibrium points, one of which is negative and has no meaning in the biological field, and two are positive, one of them is stable which verifies $\zeta'(L^*) < 0$ the other one is unstable.
 - the equilibrium point $E^* = (0, 0, 0)$ is LAS regardless of the offspring number, and we have a reason to say that it is GAS for a small number of offspring number.
 - The first equilibrium point $EE_1^* = (L_1^*, M_1^*, F_1^*) < 0$, it is negative (to be neglected), called the extinction equilibrium point, and it has no meaning in the biological field.
 - For the second equilibrium point $EE_2^* = (L_2^*, M_2^*, F_2^*) > 0$ with $\zeta'(L_2^*) > 0$, we have then an equilibrium point that is not stable
 - Lastly for third equilibrium point $EE_3^* = (L_3^*, M_3^*, F_3^*) > 0$ with $\zeta'(L_3^*) < 0$, we have then a LAS stable equilibrium point.
- Let $N > N^*$: then we have no intersection we consider $E^* = (0, 0, 0)$ as the only equilibrium point and it is LAS

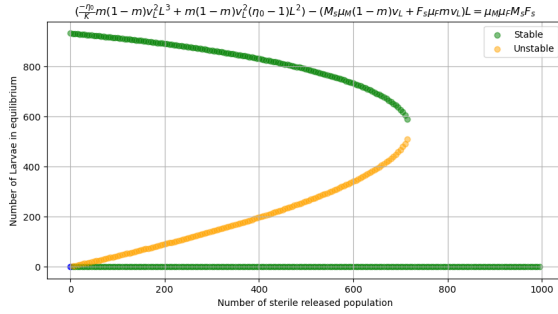


Figure 3.19: Equilibrium points and its stability in the function of the number of released population $N = F_s + M_s$ and $F_s = M_s$, first data set

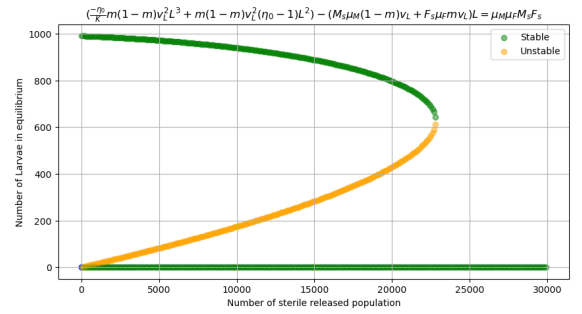


Figure 3.20: Equilibrium points and its stability in the function of the number of released population $N = F_s + M_s$ and $F_s = M_s$, second data

3.2.2 Simulation

We have illustrated in the two graphs 3.17, and 3.18, the intersection between the two curves $\zeta(L) = -m(1-m)\frac{\eta_{08}}{K}v_L^2(L^*)^3 + m(1-m)v_L^2(\eta_{08}-1)(L^*)^2$ in red, and $\Gamma(L) = [M_s\mu_M(1-m)v_L + F_s\mu_F m v_L]L + M_s F_s \mu_M \mu_F$, this intersection represents the equilibrium points depending on the number of the released population, we can notice that we have either, no equilibrium points but the trivial one, or two equilibrium points and the third one is the trivial one,

The numerical analysis of the equilibrium in 3.19 and 3.20 follows what has been proved analytically, we can see that the trivial equilibrium point is always stable, while the two positive roots, as long as they exist, one of them is stable (green), while the other one is not (yellow). After a certain number of released populations $N > N^*$ the only root we got, besides the 0, is a complex root, which we don't count as a tangible root in our study so we neglect it.

The results represented in the figure 3.23 support the analytical ones. Consequently, by choosing $N = 1000$, with the first data set, we will have eradication of the population, while such a number is insufficient even to suppress the population in the second data set and the population dynamics will converge to the greatest equilibrium point which is in that case represented by a number of larvae that is close to $L = 1000$.

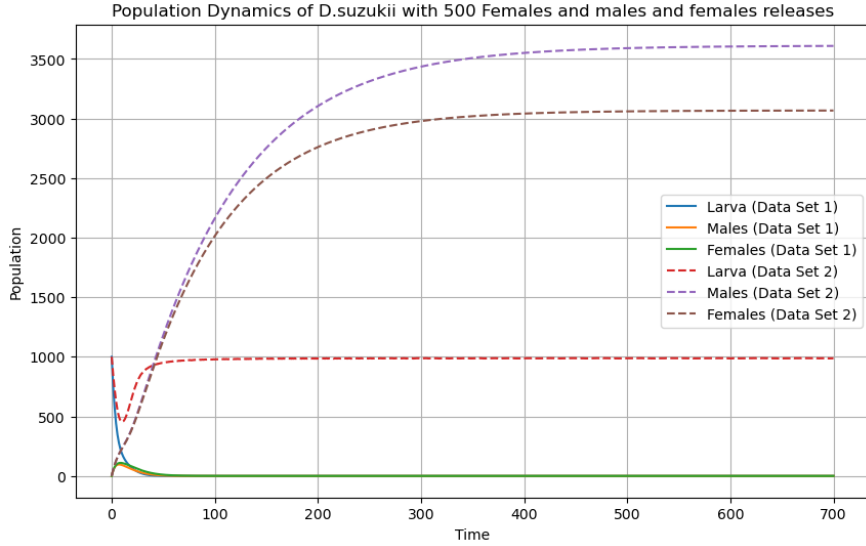


Figure 3.21: Simulation of the population evolution of *Drosophila suzukii*, in the TIS model 3.7, with continuous releases of sterile males and females ($M_s = F_s = 500$, and initial conditions of $L = 1000$, $M = F = 0$)

3.2.3 Releasing the Entire Population 7-compartment model.

Having explored various aspects of model 3.7, in the following we focus on an enhanced formulation using a broader spectrum of dynamics. The evolved model, expressed by the subsequent series of equations 3.11, is a development of the model 3.3 while inserting sterile females.

$$\begin{cases} \dot{L} = \beta \left(1 - \frac{L}{K}\right) F - (\mu_L + v_L) L \\ \dot{M} = v_L m L - \mu_M M \\ \dot{V} = v_L (1 - m) L - \left(\mu_F + v_F \left(\frac{M_s}{M+M_s} \frac{V}{V+F_s} + \frac{M}{M+M_s} \frac{V}{V+F_s}\right)\right) V \\ \dot{S} = v_F \frac{M_s}{M+M_s} \frac{V}{V+F_s} V - \mu_F S \\ \dot{F} = v_F \frac{M}{M+M_s} \frac{V}{V+F_s} V - \mu_F F \\ \dot{M}_s = \phi_1(t) - \mu_{M_s} M_s \\ \dot{F}_s = \phi_2(t) - \mu_{F_s} F_s \end{cases} \quad (3.11)$$

For insights into the functions of S , V , and F , please refer to the preceding male release model, as outlined in equation 3.3. The additional part is the seventh dimension F_s which represents the dynamics of the released sterile females population.

NB: the S cohort doesn't interact in any other cohort and all the analysis done with the previous model 3.7, can be applied in the same way, same result, and the same simulation to this model. the only difference is having two additional compartments which are V , and S , each one of them has its dynamics, and its equilibrium point. the study of the equilibrium points will be done numerically. Therefore, instead of repeating all the results of the stability and its equilibrium including all the figures 3.17, 3.18, 3.19, and 3.20, we will dive into the simulation directly.

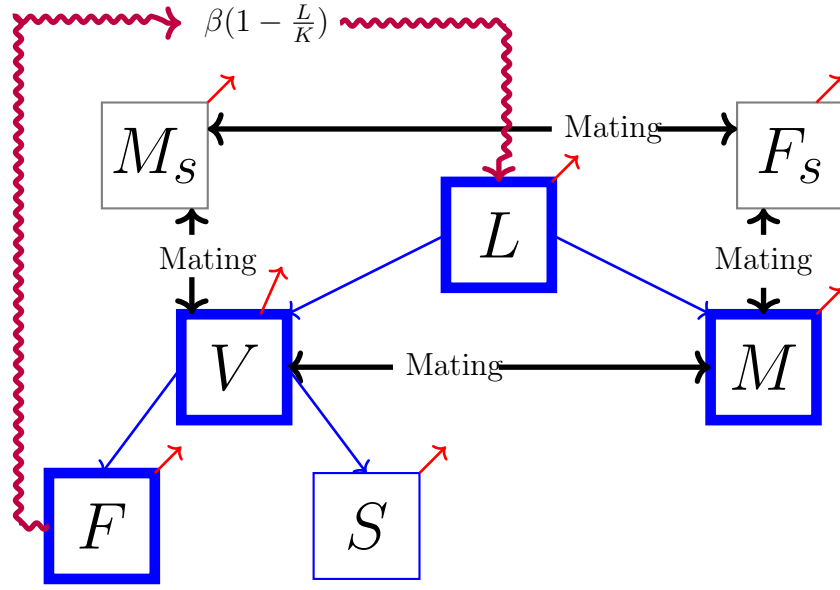


Figure 3.22: Diagram of the population model for SIT applied to *Drosophila Suzukii*, corresponding to the system of equations 3.11

Simulation

This time in the simulation we will choose another number of released populations. a number that will ensure the eradication of the population with the first dataset and the reach of a certain equilibrium point for Larvae for the second equilibrium point. For that purpose, based on the bifurcation figures 3.19, and 3.20 we will choose $N = 15000$. and we infirm throughout the simulation the results obtained analytically in the previous subsection. the only difference is the addition of a new compartment which is the S compartment, and changing the F compartment by V .

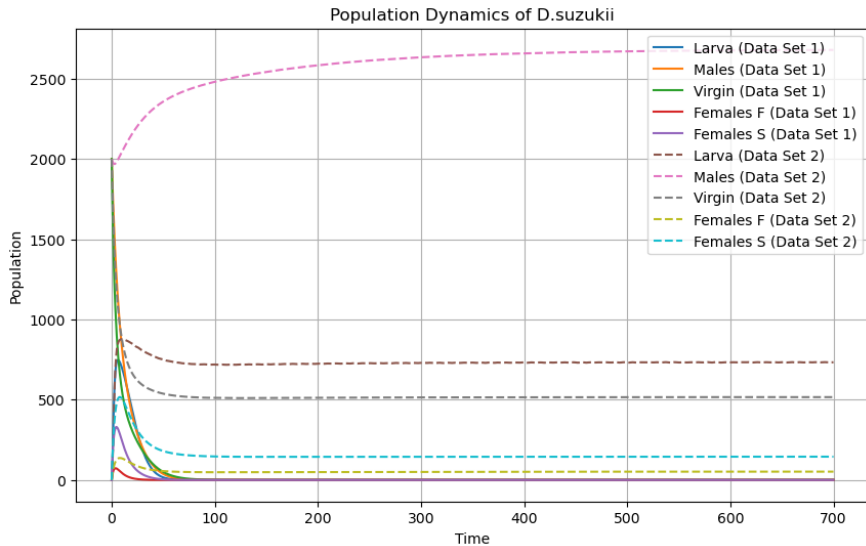


Figure 3.23: Simulation of the population evolution of *Drosophila suzukii*, in the TIS model 3.11, with continuous releases of sterile males and females ($M_s = F_s = 7500$, and initial conditions of $L = 0$, $M = V = 2000$ and $F = S = 0$)

3.2.4 The 7 compartments model with remating ability

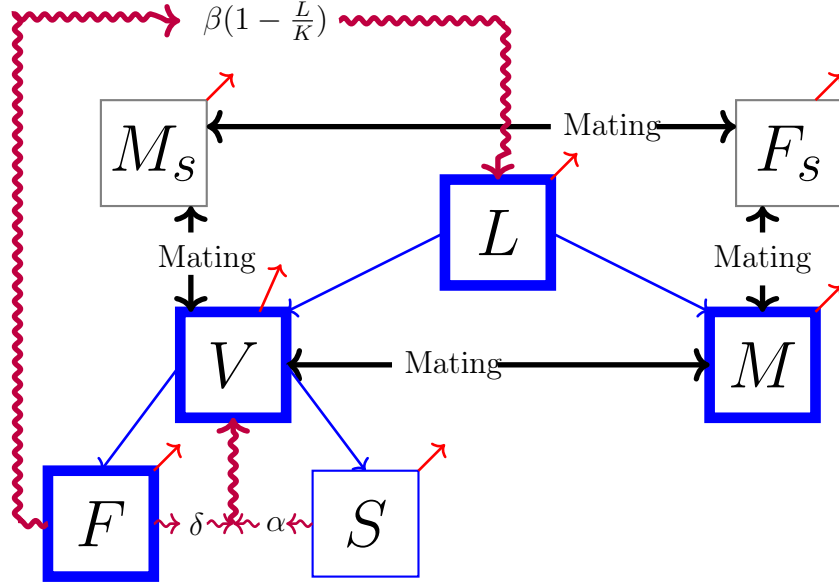


Figure 3.24: Diagram of the population model for TIS *Drosophila suzukii*, corresponding to the system of equations 3.12

The remating ability of both wild and sterile females has been described in the following model 3.12. The difference between this model and the previous one is the additional dimension described by S_s . This new dimension captures the dynamics of sterile females that have already mated. Within this context, a portion of S_s that describes the remating, denoted as α reverts to the F_s compartment. Furthermore, two additional portions of F and S , namely γ and δ , are introduced to characterize the remating potential of wild females, the probability of mating for a sterile female is described by $\frac{F_s M + F_s M_s}{V M + V M_s + F_s M + F_s M_s}$.

$$\begin{cases} \dot{L} = \beta \left(1 - \frac{L}{K}\right) F - (\mu_L + v_L) L \\ \dot{M} = v_L m L - \mu_M M \\ \dot{V} = v_L (1 - m) L + \gamma S + \delta F - \left(\mu_F + v_F \left(\frac{M_s}{M + M_s} \frac{V}{V + F_s} + \frac{M}{M + M_s} \frac{V}{V + F_s}\right)\right) V \\ \dot{S} = v_F \frac{M_s}{M + M_s} \frac{V}{V + F_s} V - (\mu_F + \gamma) S \\ \dot{F} = v_F \frac{M}{M + M_s} \frac{V}{V + F_s} V - (\mu_F + \delta) F \\ \dot{M}_s = \phi_1(t) - \mu_{M_s} M_s \\ \dot{F}_s = \phi_2(t) + \alpha S_s - \left(\mu_{F_s} + v_F \left(\frac{M_s}{M + M_s} \frac{F_s}{V + F_s} + \frac{M}{M + M_s} \frac{F_s}{V + F_s}\right)\right) F_s \\ \dot{S}_s = v_F \frac{F_s M + F_s M_s}{V M + V M_s + F_s M + F_s M_s} F_s - (\mu_F + \alpha) S_s \end{cases} \quad (3.12)$$

To investigate the impact of remating on the population, we will proceed directly to the simulation phase. A previously explored hypothesis concerning male releases, as outlined in a model 3.5, indicates that a remating ability necessitates an increased frequency of releases within the population to achieve eradication. This phenomenon will be the focal point of our forthcoming simulation study.

Simulation

In this part, we will use the same simulation as in the previous section the only difference is that we will make the assumption that the wild females mate once and the number of releases is constant throughout time.

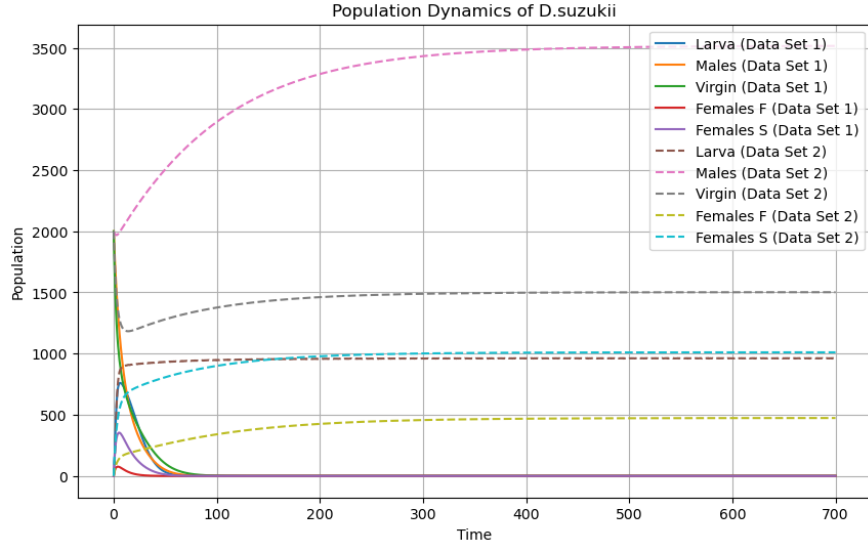


Figure 3.25: Simulation of the population evolution of *Drosophila sukuzii*, in the TIS model 3.11, with continuous releases of sterile males and females ($M_s = F_s = 7500$, and initial conditions of $L = 0$, $M = V = 2000$ and $F = S = 0$)

The impact of remating becomes evident upon comparing figures 3.23 and 3.25. In the second dataset, the Larvae population's equilibrium point has reached 800 without the remating ability. However, with the inclusion of remating ability, the equilibrium point has nearly reached 1000. This difference occurs despite the consistent release of the same number of sterile individuals. Thus, a need for more release numbers to attain the same control effect as the previous model.

3.2.5 Releasing the entire Population with preferences.

In the previous models, we have assumed that males and females, either sterile or wild, attract each other equally. For instance, a wild female cannot distinguish between a wild and a sterile male and will mate with them with an equal probability. However, these assumptions don't represent reality, and most probably both sterile males and females suffer from a lack of competition and attractiveness ability, compared to wild ones.

The presence of preferences impacts the dynamics of mating, a factor that will be incorporated into the upcoming model referenced as equation 3.13. Of course, adding the preferences will push us to change the equations 3.12 we already dealt with. The parameter β in 3.13 finds its role as a descriptor of the specific attraction that one population segment holds for another. For instance, β_{FM} symbolizes the inclination of wild females towards wild males.

This final model 3.13 incorporated many hypotheses such as the re-mating ability, the preferences, and also the dynamics of the sterile population, S_s here represents sterile females mated, the addition of this compartment will give the sterile females the mean to re-mate in the following model.

$$\begin{cases} \dot{L} = \beta \left(1 - \frac{L}{K}\right) F - (\mu_L + v_L) L \\ \dot{M} = v_L m L - \mu_M M \\ \dot{V} = v_L (1 - m) L + \gamma S + \delta F - (\mu_F + v_F (P_{VM_s} + P_{VM})) V \\ \dot{S} = v_F P_{VM_s} V - (\mu_F + \gamma) S \\ \dot{F} = v_F P_{VM_s} V - (\mu_F + \delta) F \\ \dot{M}_s = \phi_1(t) - \mu_{M_s} M_s \\ \dot{F}_s = \phi_2(t) + \alpha S_s - (\mu_{F_s} + v_F (P_{F_s M} + P_{F_s M_s})) F_s \\ \dot{S}_s = v_F (P_{F_s M} + P_{F_s M_s}) F_s - (\mu_F + \alpha) S_s \end{cases} \quad (3.13)$$

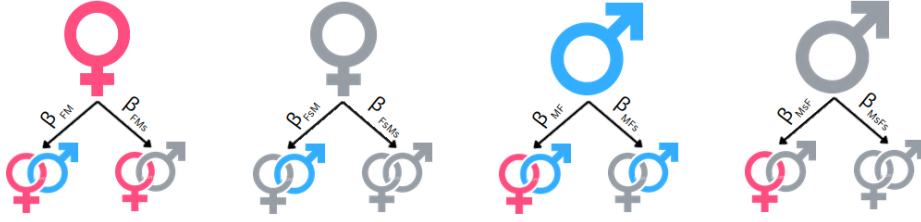


Figure 3.26: Intersexual Attractiveness of the population, grey represents steriles

The explicit form of the probabilities in the system 3.13 has not been provided due to their lengthy nature. The explicit form of mating probabilities taking preferences into account are:

- mating between **wild population**:

$$P_{VM} = \frac{\beta_{VM} M \beta_{MV} V}{\beta_{VM} M \beta_{MV} V + \beta_{VM_s} M_s \beta_{M_s V} V + \beta_{F_s M} M \beta_{M F_s} F_s + \beta_{F_s M_s} M_s \beta_{M_s F_s} F_s}$$

- mating between **sterile males**, and **wild females**

$$P_{VM_s} = \frac{\beta_{VM_s} M_s \beta_{M_s V} V}{\beta_{VM} M \beta_{MV} V + \beta_{VM_s} M_s \beta_{M_s V} V + \beta_{F_s M} M \beta_{M F_s} F_s + \beta_{F_s M_s} M_s \beta_{M_s F_s} F_s}$$

- mating between **sterile females**, and **wild males**

$$P_{F_s M} = \frac{\beta_{F_s M} M \beta_{M F_s} F_s}{\beta_{VM} M \beta_{MV} V + \beta_{VM_s} M_s \beta_{M_s V} V + \beta_{F_s M} M \beta_{M F_s} F_s + \beta_{F_s M_s} M_s \beta_{M_s F_s} F_s}$$

- mating between **sterile population**:

$$P_{F_s M_s} = \frac{\beta_{F_s M_s} M_s \beta_{M_s F_s} F_s}{\beta_{VM} M \beta_{MV} V + \beta_{VM_s} M_s \beta_{M_s V} V + \beta_{F_s M} M \beta_{M F_s} F_s + \beta_{F_s M_s} M_s \beta_{M_s F_s} F_s}$$

The explicit analysis of the model 3.13 is hard to do and because of lack of time, we will proceed directly to the dynamic population simulation given all these hypotheses.

Simulation

The simulation was conducted with a bias to mate with the wild counterparts, here the preference for a wild partner was three times greater than that for a sterile partner. For instance, regardless of whether a male is sterile or not, he finds a wild female three times more attractive and exhibits a preference for mating with her.

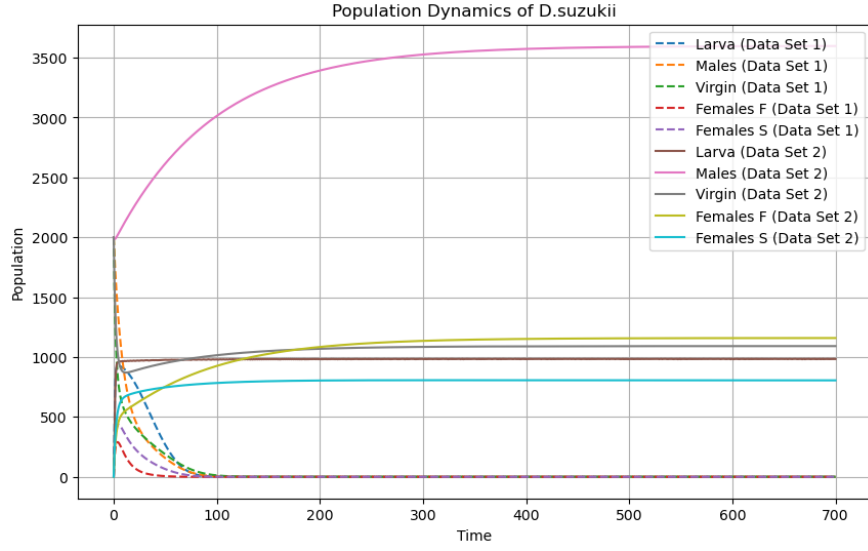


Figure 3.27: Simulation of the population evolution of *Drosophila suzukii*, in the TIS model 3.12 with preferences, with continuous releases of sterile males and females ($M_s = F_s = 7500$, and initial conditions of $L = 0$, $M = V = 2000$ and $F = S = 0$)

Parameter	Description	Unit	Data set 1	Data set 2
β	Intrinsic egg laying rate	Female ⁻¹ day ⁻¹	9	6
\mathbf{m}	Female to male ratio	-	0.5	0.5
K	Carrying capacity	-	1000	1000
μ_L	Mortality rate in the L compartment	Day ⁻¹	0.12	0.015
μ_F	Mortality rate in the V , V_s and F compartments	Day ⁻¹	0.08	0.012
μ_M	Mortality rate in the M compartment	Day ⁻¹	0.11	0.01
v_L	Transfer rate from L to V or M	Day ⁻¹	0.078	0.078
v_F	mating rate	Day ⁻¹	0.6	0.6
δ	Transfer rate from F to V	Day ⁻¹	0.1	0.1
γ	Transfer rate from V_s to V	Day ⁻¹	0.1	0.1
α	Transfer rate from S_s to F_s	Day ⁻¹	0.1	0.1
λ	Females fertilized by a single male	-	4	4

Table 3.1: Description of parameters.

The effectiveness of releasing sterile females alongside sterile males vs. only males release

This chapter is about exploring the effectiveness of each release strategy numerically and concluding the best release strategy and the optimal release to reach eradication.

4.1 Comparing the release strategies and their effectiveness in the case of the three cohort model 3.1, and 3.7

Male releases

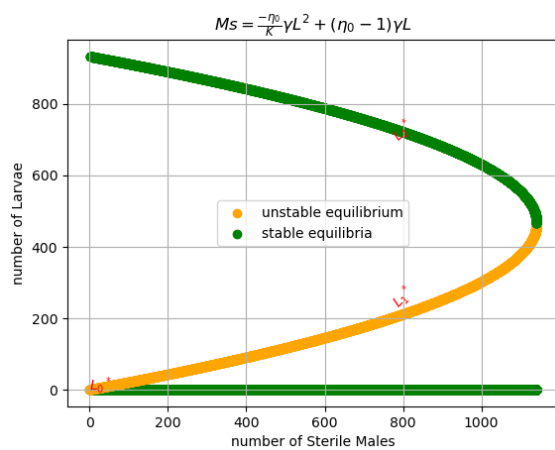


Figure 4.1: Bifurcation diagram of the stability points for the equilibrium points with SIT as a function of the number of sterile males M_s first data

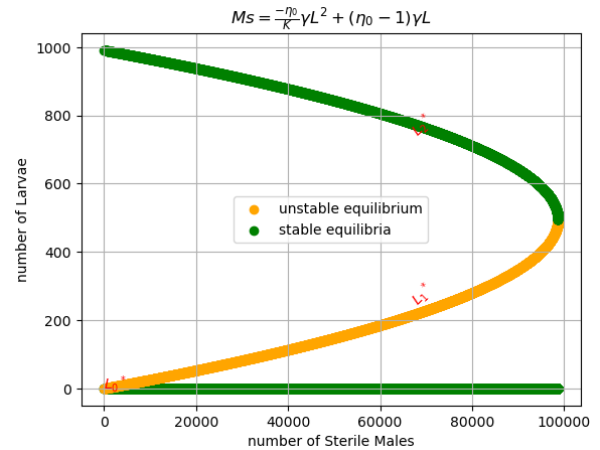


Figure 4.2: Bifurcation diagram of the stability points for the equilibrium points with SIT as a function of the number of sterile males M_s second data

Male and Female releases

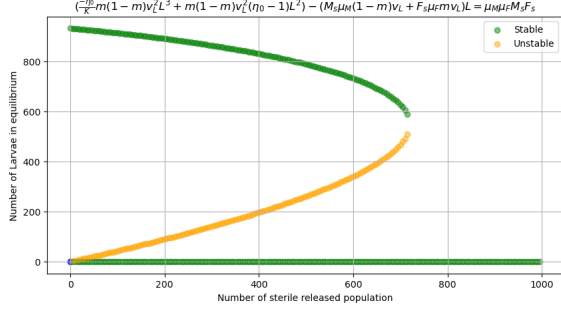


Figure 4.3: Equilibrium points and its stability in the function of the number of released population $N = F_s + M_s$ and $F_s = M_s$, first data set

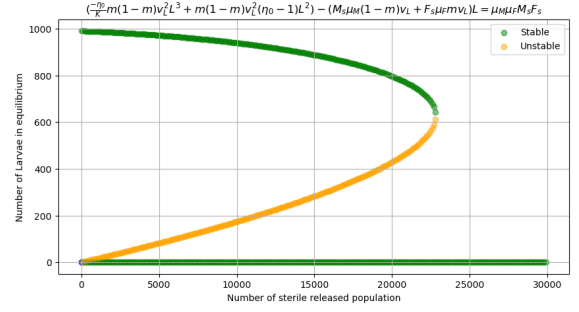


Figure 4.4: Equilibrium points and its stability in the function of the number of released population $N = F_s + M_s$ and $F_s = M_s$, second data

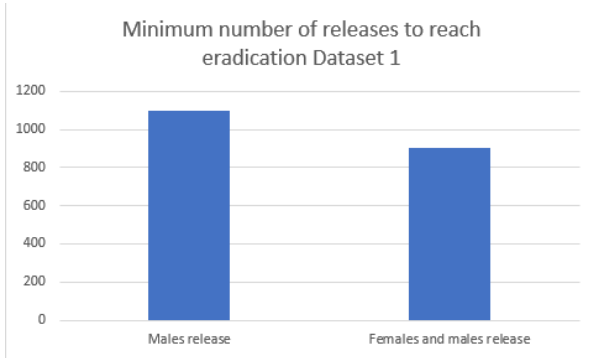


Figure 4.5: Minimum number of sterile individuals released required to reach eradication in each strategy in the first dataset

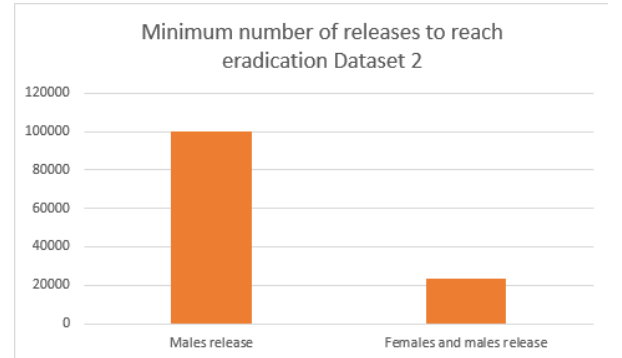


Figure 4.6: Minimum number of sterile individuals released required to reach eradication in each strategy in the first dataset

NB: Please note that whenever I mention "eradication," it is linked to the context of a small wild population.

Sterile releases of both females and males outperform the alternatives in terms of the release number of sterile. In figure 4.1 backed up by figure 4.5 with the first data set, achieving the sole trivial equilibrium point requires over 1100 sterile males. This equilibrium point's Local Asymptotic Stability (LAS) implies that for a small population of *D. suzukii* we can lead the population to eradication. However, bifurcation figure 4.3 illustrates that approximately 700 individuals released (half sterile males and half sterile females) collectively are needed to attain the GAS equilibrium point. Consequently, a combined release strategy proves more efficient in terms of the number of individuals released. Furthermore, the second dataset not only reinforces the conclusions drawn from the first dataset but also highlights the profound effectiveness of combined releases in terms of the number of individuals released. In contrast to the requirement of releasing over 100,000 sterile males depicted in figure 4.1, and shown clearly in figure 4.6, achieving eradication only necessitates the release of 20,000 sterile individuals when employing a mixed population release strategy, as depicted in figure 4.3.

4.2 Comparison of the release strategy and its effectiveness in the case of all the hypotheses included systems 3.5, and 3.12

The following two figures 4.7, and 4.8 are the simulation of the system 3.5, and 3.12 respectively, and they illustrate the release of only males 4.7, and both males and females release 4.8, within both datasets, with a remating ability for females.

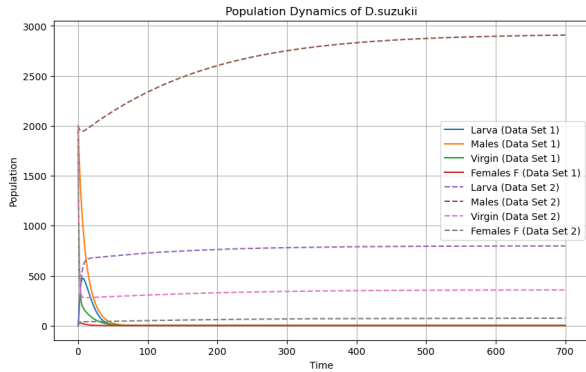


Figure 4.7: Simulation of the population evolution of *Drosophila suzukii*, in the TIS model 3.5, with continuous releases of sterile males ($M_s = 80000$, and initial conditions of $L = 0$, $M = V = 2000$ and $F = S = 0$)

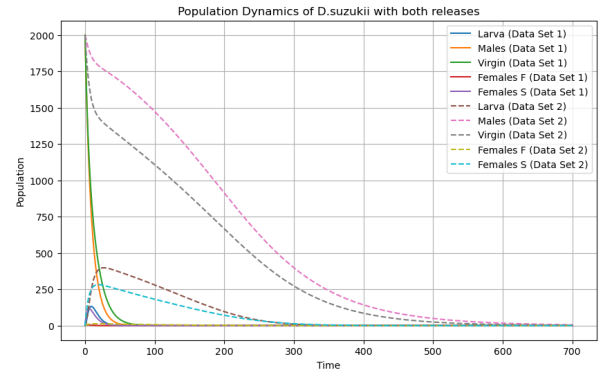


Figure 4.8: Simulation of the population evolution of *Drosophila suzukii*, in the TIS model 3.11, with continuous releases of sterile males and females ($M_s = F_s = 40000$, and initial conditions of $M = V = 2000$, and $L = F = S = 0$)

Comparing both figures we can assess the effectiveness of both releases, with a release of $M_s = 80000$ sterile males, figure 4.7, we can ensure the eradication of the first dataset population. However, for the second data, the population tends to the second positive equilibrium point.

The simulation in figure 4.8 shows that with a mixed release of $N = 80000$ sterile males and females, we can eradicate *D.suzukii*'s population using both datasets which shows the effectiveness of mixed releases.

4.3 Conclusion and Discussion

Our aim in this work is to assess the effectiveness of a mixed release of both males and females through the sterile insect technique (SIT) and compare it to the males-only release strategy.

It is worth noting that my research has faced certain challenges and complexities, such as accurately modeling female behavior and mate choices, as well as considering the potential interactions between released and wild females. However, addressing these challenges and understanding the population dynamics can be highly valuable for designing more effective and targeted pest management strategies.

In order to develop SIT for *D. sukukii* we need to know its dynamic without control. First, we initiated our work by constructing a 3-dimensional ordinary differential equation (ODE) that simulates the population dynamics of *D. sukukii* (system 2.1), the analysis has proved the existence of two equilibrium points and their stability depends on the value of the offspring number. The previous model has been developed to have a 4-dimensional model that satisfies the remating ability (system 2.7). The analysis and the simulation prove that the remating has an impact on the population dynamics.

These models enabled the simulation of sterile insect releases. Initially, we proposed the 3-dimensional model with the sterile male release as mating disruption agents 3.1. The analysis highlighted a threshold for the number of released populations M_s^* necessary to achieve population stability or extinction. This analytical study was illustrated by numerical simulations.

building upon the previous analysis, the model 3.1 was developed to have the secondary model 3.3 with more dimension in order to add the effect of remating. Despite the changes the simulation and the analysis remain consistent with the model 3.1, since we have the same dynamics of both males and larvae. The only change resides in the female dynamic that this time has divided into V , S , and F .

The effect of remating is added in the model that follows it, resulting in a more complex 4-dimensional model (Equation 3.5). The effect of remating on the population was investigated through the analysis and the simulation, the result indicates that we need to increase the threshold of releases in order to reach the control of the population.

To compare release strategies, we continue the same sequence of modeling starting with the 3-dimensional model 3.7 with sterile males and females injected in the system, then we followed the same logic by additional dimensions in 3.11 and then inserting the remating ability in 3.12. The analysis of the first 3-dimensional model 3.7 indicates that both male and female releases outperformed male-only releases, and these analyses are supported by the simulation, and we believed that both releases are more effective even with the remating ability 3.12, that's what has been shown in the simulations that have been made. However, in order to affirm what is in the simulation, a mathematical analysis is needed. Unfortunately, such an analysis couldn't be done due to the complexity and time required.

Furthermore, the study also explored the influence of mating preferences on population dynamics (Equation 3.13). The hypothesis that the population, whether sterile or wild, prefers mating with wild counterparts due to increased fitness and attractiveness was considered, this effect will render our technique more difficult to be effective and we need more releases to achieve the results already made.

It is important to know also that the SIT's effectiveness could vary depending on its implementation scale. While it might not work well when applied over large territories, it can still be successful in enclosed environments like greenhouses or net-protected plots. Specifically, when dealing with the fruit fly species *D.suzukii*, which breeds year-round on many wild plants, SIT could be a suitable method of control in those limited and contained settings^[31].

Overall, my research on modeling *Drosophila Suzukii*'s population dynamics while releasing females with males represents an exciting advancement in the field. It has the potential to enhance our understanding of the SIT technique and its application for the control of this economically significant pest species.

Future work will involve completing the theoretical analysis of the TIS model for both systems 3.11 and 3.12, studying their equilibrium points and their global stabilities, and then repeating the same process by integrating migrations. Finally, since field experiments are hard to follow due to many factors including migration, it would be interesting to use experiments in controlled conditions, such as greenhouses, to validate the results we have obtained to see the effectiveness of the mixed release.

Bibliography

- [1] Barret M. Bardin M. Jacquin-Joly E. Malausa T. Lannou C. Rusch, A. Extended biocontrol. 2022.
- [2] Derek Farnsworth-Jeffrey C Williams Frank G Zalom Rachael E Goodhue, Mark Bolda. Spotted wing drosophila infestation of california strawberries and raspberries: economic analysis of potential revenue losses and control costs. *Springer*, 04 August 2011.
- [3] Stephanie Bloem Kenneth A. Bloem Stephen D. Hight, James E. Carpenter. Developing a sterile insect release program for cactoblastis cactorum (berg) (lepidoptera: Pyralidae): Effective overflooding ratios and release-recapture field studies. *Environmental Entomology*, page 850–856, 2005.
- [4] C.Grace D.Miyashita D.O. Mcinnis, S.Tam. Population suppression and sterility rates induced by variable sex ratio, sterile insect releases of ceratitis capitata (diptera: Tephritidae) in hawaii. *Annals of the Entomological Society of America*, 1994.
- [5] D.LANCE P.RENDO, D.MCINNIS and J.STEWART. Medfly (diptera: Tephritidae) genetic sexing: Large-scale field comparison of males-only and bisexual sterile fly releases in guatemala. *ECOLOGY AND Entomology*, 97, 2004.
- [6] G. AILAM and RACHEL GALUN. Optimal sex ratio for the control of insects by the sterility method. *Annals of the Entomological Society of America*, 60:Pages 41–43, 1 January 1967.
- [7] Mello Garcia Flávio Roberto. Drosophila suzukii management. 2020.
- [8] Gabriella Tait et al. Drosophila suzukii (diptera: Drosophilidae): A decade of research towards a sustainable integrated pest management program. 123:107701, September.
- [9] Anfora G. Cini A, Loriatti C. A review of the invasion of drosophila suzukii in europe and a draft research agenda for integrated pest management. bull insectology. 2012; 65: 149–160. *Physical review letters*, 123:107701, September 2019.
- [10] Alexandra P.Krüger Monica L.Blauth Marco S.Gottschalk Flávio R. M. Garcia Luana A.dos Santos, Mayara F.Mendes. Global potential distribution of drosophila suzukii (diptera, drosophilidae). *Physical review letters*, 123:107701, September 2019.
- [11] Robinson AS Dyck VA, Hendrichs; J. Sterile insect technique: principles and practice in area-wide integrated pest management. *Springer*, 2005.
- [12] Jeffrey R. Powell. Mosquito-borne human viral diseases: Why aedes aegypti? *Applied Mathematical Modelling*, Mar. 2018.
- [13] E. F. Knipling. Possibilities of insect control or eradication through the use of sexually sterile males1. *Journal of Economic Entomology*, vol. 48, no. 4:pp. 459–462, 1955.

- [14] J. Hendrichs A. Dyck and A.S. Robinson. Sterile insect technique: Principles and practice in area-wide integrated pest management. *Springer*, 2005.
- [15] Tsuguo; Matsuyama Takashi; Sadoyama Yasutsune; Kawamura Futoshi; Honma Atsushi; Ikegawa Yusuke; Haraguchi Himuro, Chihiro; Kohama. First case of successful eradication of the sweet potato weevil, *cylas formicarius* (fabricius), using the sterile insect technique". *Applied Mathematical Modelling*, 2022-05-12.
- [16] Futoshi; Sadoyama Yasutsune; Kinjo Kunio; Haraguchi Dai; Honma Atsushi; Himuro Chihiro; Matsuyama Takashi Ikegawa, Yusuke; Kawamura. Eradication of sweet potato weevil, *cylas formicarius*, from tsuken island, okinawa, japan, under transient invasion of males. *Journal of Applied Entomology*, Mar. 2018.
- [17] Carlos Tur Miguel Ángel Martínez María Carmen Laurín Ester Alonso Marta Martínez Ángel Martín Román Sanchis María Carmen Navarro María Teresa Navarro Rafael Argilés Marta Briasco Óscar Dembilio Ignacio Plá, Jaime García de Oteyza and Vicente Dalmau. Sterile insect technique programme against mediterranean fruit fly in the valencian community (spain). *Insects*, 2021 May 6.
- [18] Anis Ben Dhahbi et al. Mathematical modelling of the sterile insect technique using different release strategies". *Mathematical Problems in Engineering*, 2020.
- [19] H.J.Barclay. Mathematical models for the use of sterile insects, in: Sterile insect technique. principles and practice in area-wide integrated pest management. 2005.
- [20] Luca Rossini et al. “modelling *drosophila suzukii* adult male populations: A physio-logically based approach with validation”. in :insects11.11 (nov. 2020), p.751.issn:2075-4450.doi:10.3390/insects11110751.url:https://www.mdpi.com/2075-4450/11/11/751. *Physical review letters*, 123:107701, September 2019.
- [21] Luca Rossini et al. A novel modeling approach to describe an insect life cycle vis-à-vis plant protection: description and application in the case study of tuta absoluta. *Physical review letters*, 123:107701, September 2019.
- [22] Yves Dumont. Roumen Anguelov, Claire Dufourdet. “mathematical model for pest–insect control using mating disruption and trapping”. in: Applied mathematical modelling. *Applied Mathematical Modelling*, pages p. 437–457., Dec déc. 2017.
- [23] Gerald Teschl. Ordinary differential equations and dynamical systems. *American Mathematical Society*, 2012.
- [24] H.L. Smith. Monotone dynamical systems: An introduction to the theory of competitive and cooperative systems, mathematical surveys and monographs. *American Mathematical Society*, vol. 41, 2008.
- [25] J. Lubuma R. Anguelov, Y. Dumont. Mathematical modeling of sterile insect technology for control of anopheles mosquito. *Comput. Math. Appl*, 64 (3), 2012.
- [26] L.Mouton C.Stauffer K.Bourtzis K. Nikolouli, F.Sassù. Combining sterile and incompatible insect techniques for the population suppression of *drosophila suzukii*. *Journal of Pest Science*, 2020.
- [27] Lisa M.Emiljanowicz et al. Development, reproductive output and population growth of the fruit fly pest *drosophila suzukii* (diptera: Drosophilidae) on artificial diet. *Journal of Economic Entomology*, août 2014.
- [28] Jana CLee et al. Biological control of spotted-wing *drosophila* (diptera: Drosophiliidae)—current and pending tactics. 2005.

- [29] Santosh Revadi et al. Sexual behavior of drosophila suzukii. *Insects*6, mars2015.
- [30] Samuel Bowong Tsakou. Contribution à la stabilisation et stabilité des systèmes nonlinéaires : Applications à des systèmes mécaniques et épidémiologiques”. *Thèse de doct. Université Paul Verlaine - Metz*, oct. 2003.
- [31] Gibert P Meirland A Prévost G Eslin P et al Poyet M, Le Roux V. The wide potential trophic niche of the asiatic fruit fly drosophila suzukii: The key of its invasion success in temperate europe. *PLoS ONE*, November 18, 2015.